Establishing an Ex Vivo Skin-Like Microenvironment Using Hydrogels to Study Macrophage-Tumor Interactions

Establishing an *ex vivo* Skin-Like Microenvironment Using Hydrogels to Study Macrophage-Tumor Interactions

Matthew Ryan Gangl

A Thesis in the Field of Biotechnology

for the Degree of Master of Liberal Arts in Extension Studies

Harvard University

May 2016

Abstract

Cancer is among the leading cause of morbidity and mortality worldwide. The disease manifests as mutations in native cells, disrupting natural cellular proliferative and apoptotic mechanisms. Cancers form and mature in numerous tissue types. Variation between cases stems from the genes disrupted by the mutation and from the tissue in which it manifests. Despite the potential for variation, research has shown numerous features and behaviors of the disease to be conserved. Strong correlations between cancer and the nature of the immune response it elicits are an important example of a conserved component. Research concerning links between cancer and the immune system, related to both progression and treatment, has established a relationship between the disease and host defense network. In contrast to its role in fighting the disease, the immune system can aid in its progression, and is sometimes the primary cause of cancer. Research efforts establishing the oncogenesis-promoting potential of inflammation (Colotta, Allavena, Sica, Garlanda, & Mantovani, 2009; Hanahan & Weinberg, 2011) were a response to observations of increased cancer risk in chronically inflamed organs. In addition to its role in tumor development, inflammation significantly contributes in the process of tumor progression (Hanahan & Weinberg, 2011). Efforts to identify the cause of these and other tumor-promoting immune system-based features such as extracellular matrix (ECM) modifications to promote migration and acquired resistance to anti-cancer treatments have identified populations of macrophages peripheral to the tumor as the

basis for nearly all tumor promoting actions resulting from immune system dysfunction (Mantovani & Sica, 2010; Solinas, Germano, Mantovani, & Allavena, 2009).

Macrophages incorporated into the microenvironmental architecture of tumors are identified as tumor-associated macrophages (TAMs). An established TAM population is capable of masking the tumor from immune surveillance and aid in its maturation through directed modulation of the immune system. TAMs can also protect against anti-tumor treatments. The underlying mechanisms for how tumor cells modulate immune response remain unclear. This is partly due to lack of *ex vivo* models that can monitor macrophage-cancer interaction. The goal of this research project was to establish a 3D culture system reflecting features of a natural microenvironment and evaluate its potential for the study of crosstalk between TAMs and tumor cells. As modulation of immune cell activation has emerged as a potential means to target cancer cells, an established and flexible *ex vivo* model would serve as an essential tool for the development of immunotherapies for tumor treatments in future research efforts.

In order to reveal the nature of the crosstalk while maximizing the extent to which *ex vivo* observations might translate to *in vivo* mechanisms, this research relied on a TAMs-tumor relationship based on a form of melanoma. The use of melanoma was based on our ability to reproduce the ECM-based microenvironmental features of skin. Through the analysis of both melanoma and macrophage cell populations following periods of co-culture, this work endeavored to reveal key features of the mechanistic basis for tumor-directed macrophage polarization. This was achieved through the development of a custom co-culture platform, the value of which was challenged by directly comparing it against an established commercial product.

Dedication

I would like to dedicate this thesis to my project advisor, Dr. Chih-Hao Lee. The time I spent as a member of his laboratory at the Harvard School of Public Health was a remarkably rewarding experience. His patience with my early laboratory work was key to building confidence in my research potential, without which I would not have been able to grow and come to understand what it is to contribute as a member of a research team. I knew him to be an excellent teacher before working with him on this project, and his ability to direct a project in a manner that worked with my strengths was key to the progression of my work. I will forever be indebted to him and will always look back on my time in his laboratory with fondness.

Table of Contents

List of Tables

List of Figures

Chapter I

Introduction

The central feature in the research efforts reported concern the nature in which two different cell types interact upon encountering one another within a specific setting. The experimental design was heavily reliant on the construction and use of an *in vitro* co-culture system. The degree to which *in vitro* observations reflect *in vivo* features is dependent on how faithfully the system replicates *in vivo* elements. It is possible for one cell to influence another by an indirect mechanism that modifies a feature of the local environment instead of relying on a direct signal (Bolós et al., 2003; Cano et al., 2000). The effectiveness of signaling molecules used by one cell population to modify another can be reliant on features of the extra cellular environment that separates them. The nature of the ECM varies from one organ to another, and human skin is an example of an organ with unique ECM components and secondary form. The nature of the EMC and its structure is often tied to the function of the tissue it resides within. Any research effort reliant on moderately replicating the nature of a cancer-TAMs relationship within the skin must recognize what a tumor microenvironment is composed of and how it is related to the cellular and ECM construction of the local tissue.

Tumors and the Tumor Microenvironment

The main elements of a tumor microenvironment are the tumor stroma, the tissue where the tumor originates from and the different sub-compartments within the tumor itself. The tumor stroma is composed of fibroblasts, endothelial cells, immune cells, soluble molecules and the ECM surrounding and supporting the tumor. For this project, the tissue where the tumor originates from is the skin. Human skin is the second largest organ surpassed only by the vascular system, and its primary function is to protect against infection and excess water loss. It is one of the most easily damaged tissues of the human body. Function is achieved through the generation of a highly conserved and elaborate cellular and ECM construction. Mammalian skin comprises a multi-layered epithelium, the epidermis, and an underlying connective tissue, the dermis. The epidermal ECM is simply a basement membrane (BM), whereas the dermal ECM comprises fibrillar collagens and associated proteins. There is considerable heterogeneity in ECM composition within both epidermis and dermis (Watt & Fujiwara, 2011). Features of the microenvironment that stem from features within the tumor itself, such as oxygen-deprived cellular regions and pockets of dead cell debris were not a concern in this project as they reflect a more developed and larger tumor mass. These inner tumor mass features are relevant to the function of peripheral cancer cells within the tumor mass and are not believed to have any role in the signaling profiles external to the tumor mass.

Directing the formation of this multi-cellular architecture and accommodating its growth through directed degradation of the peripheral ECM while maintaining high replication rates translate to the particularly high energy demands recognized in cancer cells. The mechanisms that link cellular signal transduction and cell metabolism are

largely conserved between cancer cells and healthy cells. What sets cancer cells apart is that the recognition of and responsiveness to extracellular signals directing the metabolic profile observed in healthy cells is significantly disrupted. Cancer cells typically demonstrate greater metabolic autonomy resulting from the mutational-based chronic enhancement of select pathways (Lazar & Birnbaum, 2012). The nature of these metabolic profiles is largely conserved between cancer's various forms including melanoma. This project utilizes several genes that reflect cancer metabolism as markers of cancer-like phenotype.

The most prominent change in cancer cell metabolism is an increased glucose uptake and the utilization of aerobic glycolysis instead of oxidative phosphorylation, referred to as the Warburg effect (Warburg, 1925; Warburg, 1956a). Cancer cells also show increased use of glutamine as a key source for nidogen (Hensley, Wasti, & DeBerardinis, 2013) and have increased DNA and lipid synthesis (Baenke, Peck, Miess, & Schulze, 2013). This project was specifically concerned with features of aerobic glycolysis and lipid synthesis in accessing cancer-like behavior potential in culture systems. Increased lipid synthesis during cancer cell proliferation is in part due to growth-factor signaling suppression of β-oxidation of fatty acids (Buzzai et al., 2005; DeBerardinis, Lum, & Thompson, 2006). Lipogenic enzymes ATP citrate lyase and fatty acid synthase are induced in cancer cells, and their activity is required for proliferation (Bauer, Hatzivassiliou, Zhao, Andreadis, & Thompson, 2005; Hatzivassiliou et al., 2005; Kuhajda et al., 1994; Pizer et al., 1996). Additional commonly observed features of tumor metabolism with ties to this work include the overexpression of lipogenic regulator sterol regulatory element-binding protein 1 (Srebp-1) and adipogenic regulator

peroxisome proliferator-activated receptor γ (PPARγ). Srebp-1 overexpression is an established feature in several cancers including prostate cancer (Huang, Li, Liu, Lin, & Chung, 2012) and breast cancer (Yoon et al., 2007), while PPARγ overexpression is featured in colon adenocarcinomas (Sarraf et al., 1998) and gastric cancers (Sato et al., 2000).

The high glycolitic rates in tumors provide several advantages for the rapidly proliferating cells. A shift towards β-oxidation allows cells to the most abundant extracellular nutrient, glucose, in ATP production. Aerobic glycolysis demonstrating a higher yield of ATP per glucose consumed over oxidative phosphorylation is possible as long as the glycolytic flux is great enough (Guppy, Greiner, & Brand, 1993; Warburg, 1956b). The degradation of glucose supplies tumor cells with intermediates required in multiple biosynthetic pathways. Examples include glycerol and citrate for lipids, nonessential amino acids, ribose sugars for nucleotides, and nicotinamide adenine dinucleotide phosphate (NADPH).

Macrophages and Macrophage Polarization

Macrophages are a class of differentiated immune cells originating from the myeloid progenitors best known for their role as professional phagocytes. Macrophages are key innate immune effector cells closely related to neutrophils and dendritic cells. All three cell types originate from the same lineage and exhibit phagocytotic activity. Macrophages have mechanisms for recognizing and reacting to pathogens, which makes

them important cells of the innate immune response. Their ability to cooperate with lymphocytes makes them important to the adaptive immune response as well.

Macrophages can be further classified as either tissue resident macrophages or recruited macrophages. While tissue resident macrophages exist as terminally differentiated immune cells naturally integrated into the cellular architecture of a specialized tissue, recruited macrophages are recently differentiated cells previously existing as monocytes contained within the circulatory system. Tissue resident macrophages are embryonically derived, seeded into tissues *in utero* and maintained by *in situ* proliferation (Geissmann et al., 2010; Schultz et al., 2012). Recruited macrophages, on the other hand, are generated in response to the recognition of one of a number of different signals. An activated monocyte can migrate towards a specific cellular region and subsequently undergo proliferation and differentiation, resulting in the formation of a new macrophage. This migratory behavior is directed by signaling markers, but action of migration is largely reliant on a pattern of ECM recognition and binding. The cell-adhesion molecules known as integrins serve as the mechanical link between cell and ECM and initiate intracellular signals responsible for migration (Bauer, Hein & Bosserhoff, 2005).

Tissue resident macrophages are incorporated into the natural cellular architecture of a variety of tissues. Some of these macrophages are further classified by designations that reflect the organ or tissue type within which they are integrated. The Kupffer cells of the liver and the microglia of the brain and spinal cord are two such examples. Muscle, adipose tissue and the skin all contain populations of resident macrophages, which are generally larger than the recruited class and characterized by extensive cytoplasm and

numerous vacuoles (Gordon, 2007). While these cells retain the potential for the aggressive phagocytotic behavior typical of the recruited variety, their primary function is to aid in the homeostasis of, and communicate signals to its native tissue. Tissue resident macrophages often contribute to the homeostatic effort through the recognition and digestion of a damaged or apoptotic cell, initiating an inflammatory signaling cascade in order to recruit the complement of immune cells necessary for the repair process, tempering the response of the cells that surround it to an inflammatory signal through anti-inflammatory action, and communicating tissue action to related tissue types by surveillance and subsequent signal production (Macdonald et al., 2010). More recently, tissue resident macrophages have been recognized as directly contributing to metabolic homeostasis. The fact that they are recognized as effective at surveillance and are present in key metabolic tissues makes it easy to envision these cells serving in such an important, coordinating role. Additionally, the fact that these highly responsive and versatile immune cells are present in nearly every tissue means that a number of tissue-specific diseases have features tied to the manner in which resident macrophages within the affected tissue respond to the disease state.

Macrophages possess the capacity for precise signal recognition despite the fact that the range of unique signals they might need to respond to is so great. Macrophages are relied upon to initiate change (both local and system-wide) in some cases and to indirectly respond through the coordinated direction of one or more different cell populations in others. While this range of potential can make precisely identifying the phenotypic nature of a specific macrophage population challenging, it is possible to generalize phenotypic role and classify relative to two extreme phenotypes. The behavior

typical to each of these macrophage forms are in stark contrast. The aggressive and bold nature by which recruited macrophages clear local damage and reinforce the inflammatory signal it produced appears in opposition to the patient and tempered behavior typical of tissue resident macrophages. Regardless of how different these forms appear, tissue resident macrophages maintain the capacity to respond in both manners. The degree to which a macrophage is biased towards one extreme or the other is not easily defined, but the potential for flexibility between the two phenotypes does exist for a single macrophage. This model of macrophage activation states is known as the M1/M2 paradigm. While M1 macrophages differ from M2 macrophages in many ways (initiating signals, transcriptional profiles, etc.), both fulfill important and elaborate roles.

M1 macrophages are referred to as classically activated since they exhibit the pro-inflammatory phenotype first confirmed in macrophages. The signal interferon-γ (IFN-γ) and the detection of agonists of Toll-like receptors both promote classical activation. Lipppopolysaccharide (LPS) is capable of driving the pro-inflammatory program in macrophages as well. M1 macrophages rely on aerobic glycolysis in order to meet their metabolic demands. Markers of a classically activated macrophage include IFN-γ, interleukin-1β (IL-1β) and tumor necrosis factor α (TNFα). It is possible to attenuate M1 activation by directing the over expression of elements specific to M2-like metabolic program (Vats et al., 2006).

The M1 phenotype is generally characterized by the release of pro-inflammatory cytokines and a robust production of reactive nitrogen and oxygen intermediates. The enzymatic activity of inducible nitric oxide synthase (iNOS) is tied to reactive nitrogen intermediate production, which is why expression of the iNOS gene is relied upon as an

M1 marker. The most significant contributions made by M1 macrophages are tied to features of host defense as their pro-inflammatory phenotype is critical to many elements of the immune response including the inflammatory component of the tissue repair process, immunity to microbial pathogens and anti-tumor responses.

M2 macrophages are referred to as being alternatively activated as they exhibit an anti-inflammatory phenotype and were identified after the pro-inflammatory behavior had been established. This phenotype is normally induced by Th2 cytokines such as interleukin-4 (IL-4) and IL-13. The expression of surface receptors required for macrophage endocytosis of low-density lipoprotein (LDL) and very low-density lipoprotein (VLDL) has been linked to the process of M2 activation (Oh et al., 2012), as have enzymes with roles in the same lipid-processing activities (Huang et al., 2014). The M2 phenotype is characterized by the release of IL-10 in addition to the strong expression of arginase 1 (Arg-1) and mannose receptors (Mosser & Edwards, 2008). Alternatively activated macrophages rely on lipid catabolism as the means for satisfying their metabolic demands. As a result, genes promoting fatty acid oxidation (FAO) and mitochondrial biogenesis are upregulated relative to levels observed in the M1 phenotype. Th2 cytokine-driven M2 metabolic program is primarily a STAT6-dependent mechanism (Vats et al., 2006), with the potential for a STAT3-dependent pathway to drive the same program (Gao et al., 2014). By inhibiting FAO, it is possible to prevent M2 activation. Genes that reflect this metabolic profile include peroxisome proliferator-activated receptor-γ coactivator 1β (PGC-1β), solute carrier family 25, member 20 (SLC25a20), and succinate dehydrogenase complex, subunit A (Sdha) (Kang et al., 2008). Both macrophage galactose N-acetyl-galactosamine-specific lectin 1 (Mgl1) and

Mgl2 are accepted markers of an M2 phenotype. Mannose receptor C type 2 (Mrc2) and IL-10 are also regularly relied upon as alternatively activated markers, as is the expression of mannose receptor C, type 1 (CD206). An anti-inflammatory macrophage program plays an important role in wound healing, parasitic immunity, metabolic homeostasis, and in preventing atherosclerosis. M2 macrophages play critical roles in the process of tissue remodeling (Pena, Pistolic, Raj, Fjell, & Hancock, 2011), and serve to protect host tissue from excessive inflammatory damage (Pesce et al., 2009).

At this point, their integration into numerous organs and their ability to selectively respond to a variety of signals despite possessing a wide range of potential responses have been presented as characterizing features of macrophage flexibility. It is because of their distribution, versatility and responsiveness that macrophages play so many roles. These characteristics are also the reason why macrophages have significant ties to a range of disease states. Their extensive distribution and widespread impact reflect a heavy reliance and are also the reasons why the impact of macrophage disruption/malfunction takes so many forms and is nearly always of significant concern. Disruptions compromising phenotypic flexibility or in an unintended and sustained bias towards one form or the other were of particular interest to this project. The fact that both phenotypes are relied upon as significant features in a variety of biological operations means that the manner in which one operates relative to the other within a single process can differ from role to role. Some roles require one phenotype to dominate the other, while other roles require coordinated or sequential contributions from both macrophage forms. With the nature of each phenotype being so unique, it is easy to anticipate that the presence of the wrong form at the wrong time would represent a significantly disruptive event.

The manner in which macrophages contribute to the process of repairing a minor skin lesion changes, as the early phase of tissue repair relies on classically activated macrophages while the later phase relies on alternatively activated macrophages. The shift in activation states observed as part of the natural progression of the repair process is due in part to communication between the two forms within the wound bed. Any disruptive force to macrophage phenotype can result in a delayed or damaging force within the healing process. The persistence of an infection into the late phase of tissue repair resulting from an insufficiently strong M1 response or fibrosis caused by the excessive ECM production by fibroblasts responding to an unresolved M1 signaling profile are just two examples of disruptive events.

Macrophage disruption has the potential to directly cause damage as well. Dysregulation of iNOS expression in M1 macrophages has the potential to cause inflammatory damage, similar to that associated with atherosclerosis (Teupser et al., 2006; Thomas et al., 2007). While elevated Arg-1 expression is a highly conserved feature in functional M2 macrophages, excessive and unregulated expression is capable of impairing immunity against intracellular pathogens (El Kasmi et al., 2008). The stresses applied to metabolically active tissues caused by an increasingly obese state are capable of disrupting the ability of macrophages resident to these tissues as they attempt to fulfill their roles as metabolic regulators. Increased macrophage infiltration into white adipose tissue (WAT) is a well-established feature of an obese state (Weisberg et al., 2003; Xu et al., 2003) and reflects the lipid storage capacity in some adipocytes has been surpassed. The pattern of cell death within WAT deposits serves as an indicator of tissue damage resulting in a widespread recruitment of M1 macrophages. The presence of

classically activated macrophages within populations of compromised cells only strengthens the inflammatory signal and furthers metabolic derangement. Pro-inflammatory cytokines are capable of inhibiting insulin signaling (Gasic, Tian, & Green, 1999; Hirosumi et al., 2002; Laurencikiene et al., 2007). Chronic disruption of the balance between M1 and M2 contributes to the onset of insulin resistance (Charo, 2007; Lumeng, Bodzin, & Saltiel, 2007).

Macrophages have been and continue to be of particular importance to cancer researchers as they are capable of both anti-tumor and tumor-promoting behavior. In fact, some cancers posses the capacity to direct the behavior of nearby macrophages, causing them to function in a tumor-promoting capacity. Tumors with an established complement of tumor-directed macrophages incorporated into the maturing cellular architecture are particularly challenging to treat. TAMs provide the means for the tumor to disrupt the immune response targeting it and recover from damage caused by some cancer treatments. M2-skewed TAMs executing their proangiogenic program assist tumors in their efforts to secure energy and increase the potential for tumor migration. It is not surprising that established populations of TAMs are associated with poor prognosis in many human tumors (Balkwill, Charles, & Mantovani, 2005; Bingle, Brown, & Lewis, 2002; Pollard, 2004). The same form of extended over expression in M2 macrophages has been shown to exacerbate tumor growth (Lissbrant et al., 2000; Rodriguez et al., 2004; Zea et al., 2005).

Roles of Macrophages and Phenotypical Changes in Skin Wound Healing

In order to understand the macrophage microenvironment in proximity to a developing melanoma lesion, it is important to first establish the basic features in healthy tissue. The natural microenvironment of the skin undergoes changes as melanoma progresses, and these changes are important to recognize depending on what features of cancer one wishes to investigate. Some of these changes are similar to elements in the natural process of wound healing (Schäfer & Werner, 2008).

Human skin is composed of two layers separated by a BM. The epidermis is the outer layer while the dermis lies beneath. The cellular content of the epidermis is organized into four additional layers. Listing from the outermost to the innermost these layers include the *stratum corneum*, *stratum granulosum*, *stratum spinosum* and the *stratum basale*. The BM marks the base of the *stratum basale*. The lower dermis is organized into two regions. The papillary (or upper) dermis is in direct contact with the BM while the reticular (or deep) dermis resides below. The epidermis is composed mainly of keratinocytes, and its four layers have been defined according to changes these cells undergo as they progress outward from the *stratum basale* region. This process where keratinocytes transform during outward migration from their point of origin until being shed is more than just a way to replace cells, but an ongoing progression of terminal differentiation called keratinization. The cells of the *stratum corneum* (corneocytes) are flattened, non nucleated and tightly packed. These dead cells are filled with keratin and the limited extracellular space surrounding them is saturated with glycolipids. On average, this outermost layer is sixteen cells thick with all layers being

replaced every two weeks (Hoath & Leahy, 2003). Together these layers serve to protect against physical or chemical injury, dehydration and infection.

While these migratory keratinocytes represent the vast majority of the cell population in the epidermis, there are a handful of other cell types positioned within the keratinocyte-dominated architecture. Melanocytes, Langerhans cells and Merkel cells are regularly incorporated within the population of keratinocytes and function to compliment the process of migration and modification. Langerhans cells are similar to dendritic cells in that they have immunosurveillance and antigen-presenting roles. They are positioned in the lower 2nd or 3rd layers of the *stratum spinosum* and exist in a consistently maintained ratio of approximately 1:53 with keratinocytes (Bauer et al., 2001). Merkel cells and melanocytes are found within the mitotically active keratinocytes of the *stratum basale*. Merkel cells are mechanosensory-like cells and are observed in higher density in regions of high tactile acuity like the face or finger tips. Melanocytes are larger than the surrounding keratinocytes and have a similar structure to dendritic cells in that they are in direct contact with a number adjacent of keratinocytes. The ratio of one melanocyte to thirty six keratinocytes is highly conserved (Hoath & Leahy, 2003; Lee & Herlyn, 2007) throughout the epidermis despite the high variability of melanocyte density. A cheek can contain 2,300 melanocytes per mm^2 while a thigh can contain less than half that (1,000 melanocytes per mm^2) (Fitzpatrick & Szabo, 1959). This established cellular patterning of melanocytes and keratinocytes in the epidermis is reflective of the organ's active cellular unit termed the "epidermal melanin unit" (Fitzpatrick & Breathnach, 1963). In each unit, a central melanocyte and its associated keratinocytes coordinate proliferative and migratory behaviors through a handful of signaling mechanisms.

Basement membranes are found in multiple tissues and consist of ECM molecules combined in specialized configurations, forming structures with unique properties. Human skin's BM has four main components; laminin, type IV collagen, nidogen proteins, and the proteoglycan perlecan (Timpl & Brown, 1996). Beneath the BM is the dermal layer. The dermis consists of two regions which are the papillary (or upper) dermis and reticular (or deep) dermis. Unlike the epidermis, these two dermis regions are defined by their ECM composition and not a patterned cell architecture. The dermis is rich with collagen fibers that are mainly types I and III. A thin network of collagen fibers run through the papillary dermis, while the collagen network in the reticular region is much denser. Both layers are populated by fibroblasts, macrophages, mast cells, T and B cells, blood vessels, lymphatics and nerves. A limited population of muscles are present as well. Arrector pili muscles, responsible for the action of hair erection in thermoregulation, attach to the follicle where it crosses the basement membrane. Fat deposits are most commonly encountered beneath the reticular dermis.

Macrophages at the site of skin wound repair consist of two populations differentiated according to their location within the human body prior to the damaging event. In human skin, resident macrophages exist at a density of 1-2 per mm^2 (Dipietro, Polverini, Rahbe, & Kovacs, 1995). During the initial healing phase, this population is supplemented by recruited monocytes that differentiate into macrophages upon encountering the microenvironment typical of a skin lesion. The process of wound repair in skin is a dynamic process that can be simplified into stages of inflammation, cell proliferation, reepithelialization and local tissue remodeling. While the progression of these stages is conserved, the time required to complete each stage often varies. The

precise transitions between each phase are not easily defined as features of each often overlap (Eming, Krieg, & Davidson, 2007). The first phase of wound healing is known as hemostasis. The main features of hemostasis involve efforts to minimize blood loss and form a foundation from which the process of tissue repair can be organized on and around. Platelets assume the most active role during hemostasis. In addition to the formation of the clot, platelets provide the initial signals indicating a need for skin repair and release granules containing biologically active elements such as chemokine (C-C motif) ligand 5 (CCL5), thrombin, transforming growth factor-β (TGF-β), platelet derived growth factor (PDGF) and vascular endothelial growth factor (VEGF).

The release of these initial chemoattractants marks the start of the inflammatory stage. The first immune cells to infiltrate the wound are neutrophils, whose function is to remove foreign particles and bacteria. It takes a much longer time for a substantial population of monocytes to migrate and subsequently differentiate into macrophages. Upon reaching the wound bed, monocytes rely on migratory components expressed on the cell surface (integrin receptors and selectins) in binding to specific ECM proteins such as CAMs (Brown, 1995). Following adhesion, monocytes are stimulated by various cytokines, bacterial products and ECM components to differentiate into macrophages. The complement of cytokines present in the wound bed not only reflect those released by damaged epidermal cells and the platelets associated with the clot, but also those produced by the neutrophils. Neutrophils represent a major source of pro-inflammatory cytokines (IL-1α, IL-1β, IL-6, and TNF-α) which contribute to macrophage differentiation. Typical cytokines encountered within the wound bed include IL-4, IL-10, IFN-γ and IL-13 while LPS serves as an example of a bacterial component commonly

observed within the wound capable of initiating the process of monocyte differentiation. These specific triggering elements drive a differentiation process biased towards M1 macrophages (Hübner et al., 1996; Werner & Grose, 2003). Support for this trend in an initial bias for macrophage phenotype has been provided in observations that early (24 hours post wound) infiltrating macrophages in mice mainly (85%) display a M1 phenotype (Daley, Brancato, Thomay, Reichner, & Albina, 2010).

The fact that macrophages serve different roles during wound healing is best communicated by the shift in the dominant macrophage phenotype from M1 to M2 observed during the proliferation phase. These alternatively activated macrophages coordinate the proliferation phase of repair through the release of a handful of signaling molecules intended to influence multiple cell types. M2 macrophages direct chemotaxis and cytokine production within their population through the release of TGF-β. The new ECM is produced mainly by fibroblasts and myofibroblasts residing in the dermis. To ensure the complete and efficient formation of a new ECM, the population of fibroblasts and myofibroblasts left surrounding the wound is supplemented through the differentiation of nearby mesenchymal cells (Ross, Everett, & Tyler, 1970), an action induced in response to macrophage signals TGF-β and PDGF (Kalluri & Neilson, 2003; Werner & Grose, 2003). Both cytokines, along with fibroblast growth factor 2 (FGF2) and insulin like growth factor 1 (IGF-1), stimulate fibroblasts and myofibroblasts to produce collagen and other ECM components (Ishida, Gao, & Murphy, 2008; Vogler, Saur, Kim, Schäfer-Korting, & Kleuser, 2003; Werner & Grose, 2003). TGF-β also halts the degradation of damaged matrix by indirectly decreasing the activity of collagenase so that the new ECM to form in its place.

The cellular activities of the proliferative phase represent an immediate and prolonged increase in energy expenditure. To ensure that this energy demand is met, an angiogenic program is coordinated along with the other proliferative efforts resulting in a restoration of the microvasculature that sustained the local tissue prior to the damaging event. Macrophages induce angiogenesis immediately following recruitment to the wound bed, the predominant mechanism being production of VEGF by M2 macrophages. The degradation of ECM and the BM within and near the damaged tissue follow clearance of the wound bed (Mirza, Dipietro, & Koh, 2009). This degradation is mediated by matrix metalloproteinases (MMPs) and aided by a number of other proteases. The fourth and final phase of the repair process is referred to as the remodeling phase. Its main features include reduced cell proliferation, decreased protein synthesis, and the strengthening of the ECM through fibril replacement and increased reinforcement of fibril organization.

In late repair ECM remodeling, the changes to the collagen content of the ECM are the feature with the greatest impact and largest scope. Some existing deposits of collagen type III fibrils are replaced with stronger type I collagen. Existing collagen deposits are sometimes supplemented with type VIII collagen or modified to form more durable structures through rearrangement and/or cross-linking. MMPs and their natural inhibitors, tissue inhibitors of metalloproteinases (TIMPs), are commonly recognized as the principal mechanism for ECM degradation tied to collagen substitution or structure remodeling (Ihn, 2005). MMPs are capable of degrading all elements of the ECM as well as the BM. Increased cross-linking is regularly observed in the BM during this phase. All coordinated ECM remodeling trends towards increased organization and durability.

Fibroblasts continue to serve as the primary source for EMC components, but adjust their production to match the demand. The detection of excessive ECM elements is an effective inhibitory signal to fibroblasts, with IFN-γ and TNF-α having a similar impact.

The remaining macrophages within the wound bed directly influence on the balance between the degradation, deposition and remodeling of the ECM. Macrophages are capable of modulating the capacity of other cell types to secrete matrix-degrading proteinases. In addition, they remain a reliable source of MMPs and serine proteases throughout this final phase of tissue repair. Macrophages serve as the sole source for at least one MMP active during the remodeling process (Shapiro, Kobayashi, & Ley, 1993). Reports indicating that macrophages are capable of breaking down some matrix proteins through proteinase-mediated mechanisms (Gorden, Unkeless, & Cohn, 1974; Jones & Scott-Burden, 1979) suggest a potential direct role in degradation and remodeling efforts. They are capable of directly contributing to additional ECM deposition through the production of type VIII collagen (Weitkamp, Cullen, Plenz, Robenek, & Rauterberg, 1999).

Instances where a robust infection establishes itself within the wound bed and persists beyond the inflammatory phase into the late stage of skin repair require the successful coordination of a refined immune response initiated during the remodeling phase in order for the healing process to be resolved. Clearance of a persisting infection is accomplished through a efforts mediated by T-cells and macrophages. While the population of T-cells within the wound peak after about one week, they can be found within the scar months later. During the infection, macrophages and T-cells communicate via cytokines and induce surface receptor patterning capable of resulting in

a variety of outcomes. Macrophages then stimulate T-cell expansion and differentiation to Th1 and Th2 cells. An extended presence of a sizable population of either cell type complicate the process of remodeling as they prolong the duration of a inflammatory signal, interrupt cell migrations, and delay ECM production and represent an atypical increase in the local energy requirements during late repair. A moderate population of Th1 cells is typical of early wound repair and they direct macrophage polarization towards the M1 phenotype. Significant Th2 cell populations result in the production of ECM, which is why fibrosis and necrosis can result from prolonged infections.

The preceding outline of skin repair serves to demonstrate that macrophage cells serve a significant role throughout the process. The manner in which they contribute changes from one phase to the next, and is reflected by the nature of the population within the wound bed. Phenotypical flexibility is required for repair progression as a M1-dominated population during the inflammatory phase transitions into an M2-dominated population for the proliferation phase. Tissue resident macrophages are among the first cell populations responding to the wounding event and remain integrated within the repaired tissue long after the recruited macrophages are gone. The need for phenotpical flexibility and signal responsiveness are key to various ways macrophages influence the surrounding microenvironment during skin repair was a key theme in this research project.

Using Melanoma Cell Model to Study TAM-Tumor Interactions

Phenotypical flexibility is required for repair progression as a M1-dominated population during the inflammatory phase transitions into an M2-dominated population for the proliferation phase. This shift resembles the basic phenotypical changes observed in TAMs. As such, this project used murine melanoma cell lines and primary murine bone marrow-derived macrophages in a model system to investigate how tumor cells instruct TAMs to acquire an M2-like phenotype with a focus on STAT6 and PPAR δ/γ driven mechanisms. The difficulty in establishing a control co-culture system as part of the co-culture experimental design was resolved through the selection of a specific melanoma cell line that includes phenotypical variants as the result of directed genetic alterations. The control co-cultures relied on the use of the spontaneous mouse melanoma cell line B16F-0, served as a backdrop for observations made in co-culture with its metastatic clone B16F-10 (Fidler, 1973). B16F-10 melanoma was a product of early work concerned with identifying characteristics that translated to enhanced metastatic properties and derived from serial subcutaneous injection and selection of B16F-0 melanoma in the C57BL/6J strain of mice (Fidler, 1973). This method of selection based on metastatic ability has proven valuable to numerous cancer studies since first being described with the B16 melanoma line (Nakamura et al., 2002), and experimental designs contrasting B16F-0 and B16F-10 melanoma have been regularly relied upon (Park, Kim, & Jeon, 2012; Sabuncu, Liu, Beebe, & Beskok, 2010) subsequent to discoveries revealing the limit genetic variance between them (Melnikova, Bolshakov, Walker, & Ananthaswamy, 2004).

Importance of Reflecting Native Microenvironmental Features in *in vitro* Models

A fundamental component was establishing a three-dimensional (3D) co-culture method using hydrogels to mimic the ECM that supported tumor growth and permitted spherical-like maturation. The use of a 3D culture for studying cancer is extremely important since they are uniquely capable of showing differences in functional behaviors such as differentiation, proliferation, and gene expression when compared to cells cultured on a flat surface (2D) (Bissell & Radisky, 2001; Cukierman, Pankov, & Yamada, 2002; Erler & Weaver, 2009). These differences are tied to the fact that a 3D culture system more accurately reflects the features observed *in vivo* and is why they were so significant in the design of the co-culture system utilized in this project. Numerous examples of research efforts based on the co-culture of tumor cell lines and immune cells have been reported, but only recently has the importance of incorporating a 3D platform become generally accepted.

The value of incorporating 3D features into *in vitro* systems has been a recent theme in many fields of biological research in addition to cancer studies. Driving this trend is a growing consensus that increased reflection of microenvironmental features means *in vitro* observations are more likely to reflect *in vivo* behaviors. In many cases, 3D models provide more comprehensive and relevant biological data that is difficult or even impossible to obtain from traditional 2D systems (Ghajar & Billell, 2008; Griffith & Swartz, 2006; Nelson, Vanduijn, Inman, Fletcher, & Bissell, 2006). 3D culture platforms

are now standard for cell migration and directed cell growth studies, features of the developmental and immunological fields. In developmental biology, in vitro work concerning molecular gradients and directed cell growth require the use of 3D culture systems. Axonal growth, like tumor maturation, occurs in coordination with local ECM degradation and remodeling. The same type-I rat-tail derived collagen used in this project has been used study axonal growth (Gil & del Río, 2012) and the nature of chemorepulsion/chemoattraction. Advances in cell migration and wound-healing assays have relied on collagen type-I hydrogels (Rommerswinkel, Niggemann, Keil, Zänker, & Kittmar, 2014). Features of small-scale fabrication are easily integrated into hydrogel platforms, like the incorporation of microfluidic structures in generating artificial molecular gradients (Cate, Sip, & Folch, 2010; Goodhill & Baier, 1998; Keenan & Folch, 2008; Rosoff, McAllister, Esrick, Goodhill, & Urbach, 2005).

In cancer research, 3D culture platforms have proven value over traditional 2D culture for virtually all forms of cancer and in multiple types of investigations. Observations showing an inability to replicate the phenotypic variations within tumor architecture in terms of gene expression and differentiation, paired with a growing acceptance of the limited predictive value offered in efficacy of therapies (Hosoya et al., 2012) drove this shift towards reliance on 3D *in vitro* systems. Variations of 3D culture platforms have demonstrated value in multiple fields including tumor formation, tumor cell migration, tumor-stroma interactions, drug developments and specialized drug delivery systems.

As stated above, our understanding of how different elements of the tumor stroma contribute to cancer progression has been greatly aided by the use of ECM-like scaffold

and matrix-based 3D culture systems. Early work developing 3D culture platforms for cancer research relied on the commercial product Matrigel®, which is a biologically-derived ECM reagent. Eventually, the limited control over the physical and biological properties of the early form of this natural ECM material paired with its expense inspired the development of commercial alternatives and custom, home-made 3D culture platforms. What makes the design in this project unique is the combination of an established tumor model with a 3D co-culture platform that is both low cost and customizable in an effort to further resolve a mechanistic basis for tumor-directed macrophage phenotypic polarization.

Chapter II

Materials and Methods

The experimental design was based around identifying patterns in gene expression within specific populations of cells following rounds of culture. Gene expression in co-cultured populations was evaluated based on observations in mono-cultured populations of the same cell type. For each round of experimental culture, populations were prepared in triplicate. All work was conducted in laboratory space with the Harvard School of Public Health.

Cell Lines

The model of TAMs utilized in this project involved the co-culture of murine macrophages and murine melanoma cells *in vitro*. Primary macrophages were generated from directed differentiation of bone marrow harvested from mice of various genetic backgrounds. Melanoma cell lines designated B16F-0 (ATCC catalog CRL-6322) and B16F-10 (ATCC catalog CRL-6475) were purchased from ATCC and stored in liquid nitrogen until required. Both melanoma cell lines were generated in the murine strain

designated C57BL/6J. Cell stores were recovered and expanded as needed. Melanoma cultures were maintained and expanded on 10 cm tissue culture plates (Corning catalog 430167) in high glucose DMEM containing 10% fetal bovine serum (FBS) and 1% penicillin-streptomycin at 37°C and 5% carbon dioxide. Once plated, melanoma cultures were evaluated daily and split prior to reaching complete confluency. Cultures were typically split every 3 to 4 days.

Melanoma spheroids were generated by subjecting cell suspensions to an extended shaking at 37°C. Each 3D melanoma culture was prepared by suspending 400,000 cells in 2 ml of fresh medium and then transferring them to altered 50 ml conical tubes. These tubes had been cut to reduce their height. Decreasing the distance between the surface of the cell suspension and the top of the tube allowed for better gas exchange during the process of spheroid formation. Each tube was then secured on a plate shaker located within an incubator. Once secured, suspensions were lightly shaken for a period of 2 to 4 hours. The progress of spheroid formation was checked sometime after 2 hours to ensure all suspensions contained spheroid structures. These 2 ml suspensions were added directly to 3D culture platforms and supplemented with fresh medium. Melanoma spheroids were left to bind to their culture platform and expand before starting a new experiment.

For bone marrow isolation, RPMI containing 2% FBS was ejected from a syringe through a 25G needle. Once collected, the cells of the marrow were broken up, pelleted, and resuspended in ACK red blood cell lysis buffer. These cells were once again pelleted, resuspended in 30 ml of differentiation medium (low glucose DMEM, 10% FBS, 30% L929 conditioned medium and penicillin-streptomycin) and plated on 15 cm

petri dishes. At day 3 to 4, 20 ml of the original differentiation medium was replaced with fresh medium. Cell attachment began around day 5 and cells were harvested on day 6 to 7 depending on when attachment was observed using a cell scraper to detach the cells. Populations of macrophages were re-suspended in low glucose DMEM containing 10% FBS prior to counting cells and plating them in their final format for co-culture experiments.

Reagents for Cell Culture

All mono- and co-cultures were prepared using standard 6-well tissue culture plates (Corning catalog 3506). Collagen used in the preparation of custom melanoma culture platforms was purchased from Roche Diagnostics (catalog 11179179001) and purified from rat tails. The protocol relied upon for the resuspension, casting, curing and sterilization of collagen wells was done according to the manufacturer's instructions with slight modifications. Vials of lyophilized collagen were dissolved with 3.3 ml sterile 0.2% acetic acid (v/v), pH 3.0 introduced using a sterile syringe giving a final concentration of 3 mg/ml. Acetic acid was introduced to collagen vials at 4°C and then mixed slowly using a nutator kept in a cold room (4°C) for 2 to 3 hours.

Once the collagen was completely dissolved, vials were placed on ice and relocated so that all subsequent steps could be performed within a biosafety cabinet. Under the hood, 0.8 ml of sterile 10 X PBS (with sodium bicarbonate, pH 7.4) and 0.8 ml of 0.2 M Hepes (pH 7.3) were carefully added to vials of resuspended collagen and gently mixed via pipetting. Both 10 X PBS and 0.2 M Hepes were cooled to 4°C before

being introduced to the collagen. A volume of 960 µl of this collagen solution was added to the base of select wells in sterile 6-well tissue culture plates, achieving hydrogel coverage of 100 µl per 1 cm^2 of surface area. Plates were carefully tilted to assure complete and even coverage, resulting in a uniform base layer approximately 1 mm thick.

Immediately following well coating, collagen plates were left in the biosafety cabinet at room temperature for 15 minutes then incubated for approximately 2 to 3 hours at 37°C in a humidified atmosphere to allow for gel formation. Once the gel layers had solidified, plates were capped with their lids and sealed using plastic wrap before being stored at 4°C. Preparing plates for cell culture began with 15 minutes of exposure to U.V. light while protected within a biosafety cabinet following removal from 4°C storage. Gel coverage was re-evaluated to assure consistent quality. Gel layers were washed using 1 X PBS before equilibration. For equilibration, 2 ml of melanoma media was added to each well for a period of 15 minutes. Removal of both 1 X PBS and equilibration media was done using a manual pipette as opposed to a vacuum line to minimize the stress and avoid gel damage.

Matrigel ®(Corning® catalog 354234) was purchased from Corning®. The process of resuspending and casting Matrigel® was based on the manufacturer's protocol. Matrigel ® vials were removed from -20°C storage and thawed on ice before an extended period of careful mixing at 4°C to assure complete resuspension and a homogeneous mixture was achieved while minimizing the formation of bubbles. This was accomplished with a nutator in a cold room for a period of at least 60 minutes.

Once dissolved, vials were transferred to a biosafety cabinet and 960 µl of Matrigel ® was transferred to designated wells on 6-well T.C. plates. This achieved a

coverage of 100 µl per cm^2 in each well, matching that of the collagen wells. Plates were tilted and shaken while on ice to assure complete and even coverage before solidification began, then placed at 37°C for 30 minutes. Following this incubated curing period, plates were relocated to a biosafety cabinet and the plate lid removed briefly so the air flow assured complete drying of the Matrigel ®. The plates were then covered, sealed with parafilm, and stored over night at 4°C.

Preparations for the addition of melanoma spheroids to Matrigel ® coated wells were identical to those outlined for collagen. Plates were removed from cold storage and placed within a biosafety cabinet to slowly warm and exposed to ultra violet light for approximately 15 minutes to further prevent contamination. Each well was washed with 1 X PBS and then equilibrated through the temporary addition of melanoma media.

Macrophage populations were introduced to select wells using Transwell® inserts (Corning catalog 3414). These 24 mm diameter inserts feature sterile polycarbonate membranes with a pore size of 3.0 µm. Once collected and counted, differentiated macrophages were transferred to these inserts and given 24 hours to acclimate to the new culture surface before being introduced to select wells on the experimental plate. During this period, macrophages remained in differentiation media. A volume of 2 ml was added to each well of a 6-well culture plate before the introduction of Transwell ® inserts. The desired number of macrophages was 2 million for each individual insert. These cells were added to inserts in 1.5 ml of differentiation media and left at 37°C and 5% carbon dioxide for 24 hours.

Experimental Preparation and Design

Experimental preparations were based around macrophages since the isolation and extended differentiation process were the most demanding and least flexible features in each round of experimental culture. Macrophage differentiation required 6 to 7 days of culture. During this time, the appropriate melanoma lines were plated and maintained. To assure an excess of melanoma cells were available for each experimental round, populations were often expanded before macrophage differentiation concluded. Plates typically were coated for 3D culture 24 hours prior to differentiation then stored at 4°C.

Once isolated and counted, macrophage suspensions were modified to achieve a cell concentration of 2x10^6 per 1.5 ml. Transwell® inserts were introduced into wells containing 2.0 ml of differentiation media and then 2 million macrophage cells were added to each insert. Macrophages were left in the differentiation media to adjust to the new culture environment for 24 hours at 37°C and 5% carbon dioxide.

The appropriate collections of melanoma cells were prepared during the 24-hour period of macrophage acclimation. Once the cells in B16 suspensions had been counted, the cell numbers needed to satisfy the 3D cultures were removed, separated into 2 mL aliquots of 400,000 cells, and subjected to the 4 hour spheroid-generating treatment. Wells coated for 3D culture were sterilized, hydrated and equilibrated during the period of spheroid formation. For 2D wells, 2x10^5 cells were introduced in melanoma/co-culture media volume of 2 ml. Once the formation of spheroids was visually confirmed, 3D cultures were introduced by directly transferring the spheroid suspensions into the appropriate coated wells. Having introduced the appropriate B16 populations to the test

plates, cells were returned to 37°C and 5% carbon dioxide for the duration of the macrophage acclimation period. During this time, spheroids attached to the 3D coating and both 2D and 3D populations expanded. The number of B16 cells used for the spheroid generation and 2D cultures were selected following preliminary testing to allow for continued expansion during the 2 to 3 days that followed while avoiding the potential for the population in any well to reach confluency prior to the conclusion of the experimental culture period.

Once the macrophage-laden Transwell® inserts were ready for use, both the macrophages and melanoma plates were removed from incubation. A portion of the old co-culture media was removed and replaced in wells containing melanoma cultures, while the full volume of 2 ml was added to empty wells intended to serve as macrophage mono-cultures. Differentiation media was carefully removed from Transwell® inserts, which were then rinsed with 1 X PBS before being introduced to test plate wells. Once in place, an additional 1 ml of co-culture media was added to each insert. After confirming the absence of air bubbles beneath inserts, plates were covered and returned to 37°C and 5% carbon dioxide. This point marked the start of the experimental culture phase, which lasted for 48 hours. 1 ml of fresh media was carefully added to all wells after 24 hours and the nature of the melanoma cultures was checked under a microscope at this time as well.

RNA Isolation and Reverse Transcription

The isolation of RNA from cells following each period of experimental culture was accomplished using materials from PrepEase RNA spin kits purchased from Affymetrix (catalog 78767) and according to a protocol based on that which accompanies the kit. All experimental cell populations were kept on ice during the initial steps of cell lysis and RNA isolation.

Transwell® inserts were removed from the test plates and placed into clean wells on a fresh plate kept on ice. For inserts supporting macrophage populations, co-culture media was removed and the cells washed with 1 X PBS. To collect macrophages, kit reagent RA1 lysis buffer combined with beta-mercaptoethanol was added to washed cells and the insert carefully scraped before the lysate was collected and transferred to PrepEase filtration tubes. Control inserts used in melanoma mono-culture wells were cleaned and stored. Melanoma populations were washed and collected in the same manner except that no cell scraper was used in 3D cultures to avoid excessive hydrogel content in the lysate. Once in filtration columns, the PrepEase protocol was followed to isolate and resuspend RNA. A volume of 2 μl of resuspended RNA was collected from each tube and used to determine RNA concentration with a microdrop device. Reverse transcripts (RT) were generated using VersoRT CDNA synthesis kits purchased from Thermo Scientific (catalog AB1453A) according to the manufacturer's protocol. Isolated RNA samples were stored at -80°C.

Q-PCR

Gene expression was quantified using an Applied Biosystems StepOne Plus unit to determine SYBR Green (Invitrogen catalog S-7563) fluoresce in reaction wells on a 96-well plate. Standard dilutions of the RT products were prepared at ratios of 1:16, 1:40, 1:100 and 1:400. The primer sequences used in quantifying gene expression can be found in the supplementary data. All reactions were performed in triplicate. Outliers or failed reactions were eliminated from further analysis in the StepOne Plus software.

Statistical Analysis

Gene expression data were normalized to 36b4 expression. Standard deviations were calculated and used to determine the standard error of the mean for normalized sets of expression values. The results of the standard error of the mean are reflected in error bars. A student's t-test was used to determine significance in changes observed between sets of expression values, with a p-value less than 0.05 regarded as significant.

Chapter III

Results

The experimental design was built so that the different culture formats utilized at each phase of the project addressed a specific question. Observations were built upon in subsequent experimental phases of culture. Having established features of the cells and optimized the hydrogel preparations, the first phase of culture experiments were intended to confirm the B16F-0/10 model and that our custom 3D culture system translated to a more tumor-like population. This work was followed by a shift in focus from the tumor component to the macrophages as we evaluated the potential of the co-culture to direct macrophage phenotype and define the basic features of any change. Having determined the co-culture platform as functional, it was then directly compared against Matrigel ® systems. The final phase of experimental cultures sought to probe the mechanistic cause for this shift in macrophage phenotype.

Tumor Model

Work with the two melanoma cell lines showed both to be robust and consistent in their proliferation rates. The 2D wells of experimental plates for both B16F-0 and B16F-10 populations reached similar states of confluency during the 3 day culture period as seen in panels A and C of Supplemental Figure 1. Both cell lines were capable of forming spheroids with similar attachment behaviors. Supplemental Figure 1 also provides examples of B16F-0 and B16F-10 spheroids in panels B and D, respectively, 24 hours following introduction to collagen 3D culture. The same 4 hour period of spheroid generation treatment was sufficient for both lines. The manner in which spheroids matured during experimental 3D collagen culture were also similar. The average size of spheroids generated by each line suggested that B16-F10 may have been slightly bigger, but this pattern was not substantial or equally reflected in each round of experimental culture.

To evaluate the basic nature of the two melanoma cell lines and determine what impact the 3D culture system might have, expression of key metabolic genes was quantified in 2D and 3D mono-cultures for both lines. In B16F-10 populations, expression of lipogenic genes Srebp-1c, acetyl-CoA carboxylase 1 (ACC1) and FASN expected to be up-regulated in tumors were significantly increased in 3D collagen culture systems (Figure 1B). This pattern of increased lipogenesis in 3D culture was only partially observed in B16F-0 populations (Figure 1A). While the increased expression of FASN was significant upon 3D culture in both lines, B16F-0 ACC1 increased expression

was not significant and Srebp-1c appeared unchanged. These results suggest that B16F-10 3D cultures exhibit a metabolic phenotype similar to that of tumors.

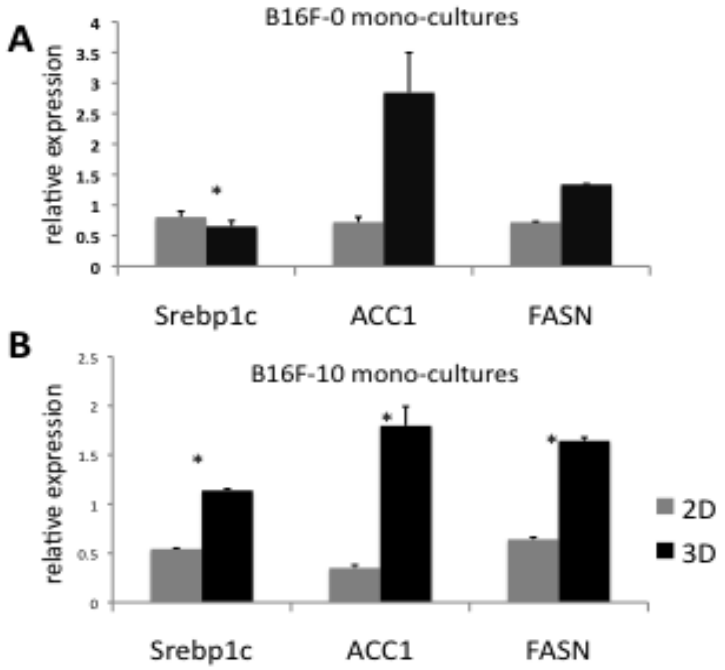

Figure 1. Metabolic gene expression of melanoma mono-cultures in 2D and 3D environments using real-time PCR. For both B16F-0 (A) and B16F-10 (B), gray reflects relative expression in 2D populations and black for 3D collagen populations following a 48 hr culture period. The * symbol indicates a p-value<0.05. It appears over Srebp1c in panel A and over all three genes in panel B.

Culture Environments and TAM Phenotypes

To test our hypothesis that macrophages would respond with an M2-biased phenotypic shift when co-cultured with tumor-like populations, gene expression in WT macrophages combined with B16F-10 3D collagen populations was determined and compared against WT macrophage mono-cultures. The results reported in Figure 2

reflect a probable increase in Mgl1 expression and a significant increase in Vegfα expression were observed in WT macrophages following a period of co-culture, indicating an M2-like phenotype.

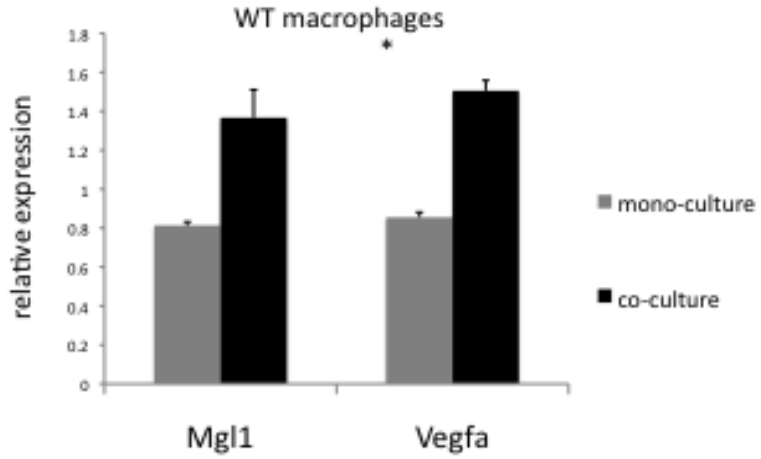

Figure 2. Effect of co-culture with melanoma on macrophages using activation marker expression determined by real-time PCR. WT macrophages were cultured with 3D B16F-10 collagen populations or alone for a 48 hour period. Relative gene expression between the two culture conditions is presented, with the "*" symbol over Vegfa indicating a p-value <0.05.

To further investigate the nature of macrophage changes resulting from melanoma co-culture and attempt to identify signaling mechanisms responsible for the M2-like activation, additional macrophage cell lines were incorporated into culture experiments. Pairings of mono- and co-cultured WT macrophages were replicated using macrophages from myeloid specific deletion of PPARδ/γ KO or STAT6KO genes, both of which have been implicated in M2 polarization of macrophages. Gene expression is reflected in Figure 3.

As expected, WT macrophages co-cultured with B16F-10 spheroids expressed a higher level of M2 markers, including Mgl1 and Arg-1, and a lower level of M1 markers, such as TNFα (Figure 3). Similar results were observed in STAT6KO cells, indicating STAT6 is not required for the TAM phenotype. In contrast, there was a reduced response in the expression of Mgl1 and TNFα in PPARδ/γ KO macrophages. These results suggest that the nuclear receptors PPARδ and PPARγ may mediate certain aspects of TAM polarization.

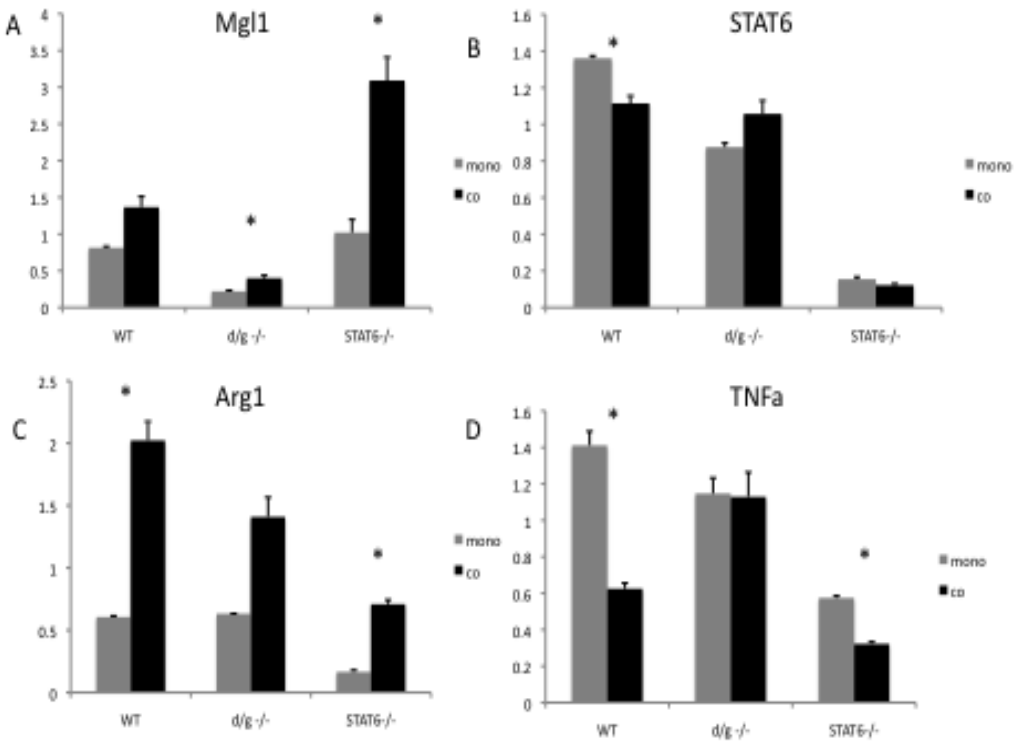

Figure 3. The PPARδ/γ and STAT6 nuclear signaling KO macrophage lines were incorporated into the mono- (gray) and co-culture (black) system pairings along with WT macrophages, then harvested after 48 hour period. Panels (A) through (D) report cumulative gene expression figures in each population of macrophages. In each panel, the cell lines represented are WT, PPAR$^{\delta}$/γKO and STAT6KO from left to right.

Comparison of Coating Materials

Having tested the custom 3D collagen-coated co-culture system's basic potential in serving as a platform for TAMs research, we shifted the experimental design to

directly compare our system to Invitrogen's Matrigel ®. Attachment of all B16F-10 spheroids after 24 hours of culture was observed in Matrigel ® wells just as with collagen. The manner in which 3D B16F-10 cultures matured following hydrogel attachment differed between the coatings. Nearly all growth of spheroids cultured in collagen hydrogel occurred above the coating with some expansion along the surface for increased adhesion. In Matrigel ® cultures, spheroid expansion demonstrated infiltration of the hydrogel as wells as producing larger tumor-like clusters above the interface stemming from points of spheroid adhesion. Examples of these melanoma maturation phenotypes are provided in Supplemental Figure 2. After 24 hours of culture, the average size of collagen spheroids (Supplemental 2A) was greater than those in Matrigel ® (Supplemental 2B). Melanoma hydrogel infiltration was observed in Matrigel® at this time, in the form of elongated growths extending from the periphery of attached spheroids (Supplemental 2B). These structure were completely absent in collagen cultures (Supplemental 2A). These features of larger B16F-10 3D structures in collagen (Supplemental 2C) and significant hydrogel infiltration in Matrigel ® (Supplemental 2D) were far more pronounced following an additional 48 hours of culture. Melanoma infiltration into collagen hydrogel was observed in some wells, but not to the extent typical of Matrigel® cultures.

The gene expression comparison in terms of B16F-10 spheroid culture, reported in Figure 4, offers some support to these unique features of population maturation in Matrigel ® cultures. The trend observed in most metabolic markers tested show a more tumor-like lipogenic profile demonstrated in the commercial hydrogel.

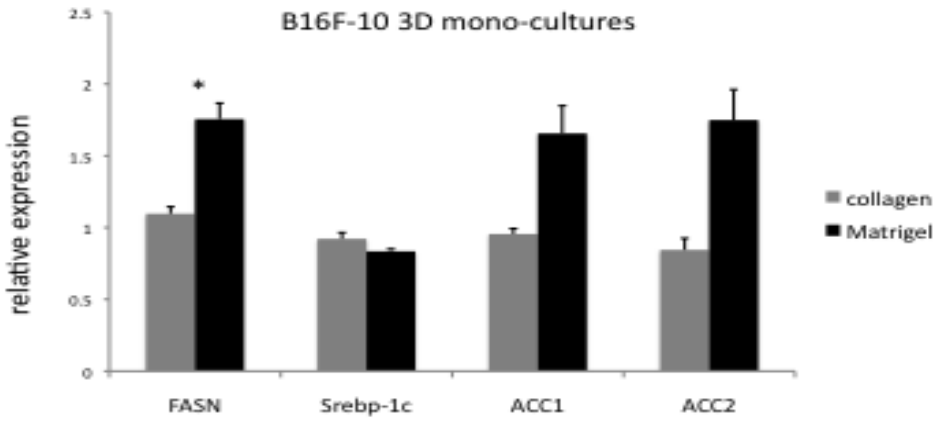

Figure 4. The effect of hydrogel platform on the tumor-like nature of B16F-10 spheroid cultures. Gene expression of B16F-10 mono-cultures was used to compare custom collagen platform and commercial Matrigel® systems. The "*" symbol reflects a p-value below 0.05, and appears only over FASN

Gene expression in WT mono-cultured macrophages versus populations co-cultured with melanoma was used to compare the two hydrogel platforms. Observations of increased macrophage Arg-1 expression in response to co-culture for collagen systems was conserved, with Matrigel® systems demonstrating an identical change (Figure 5B). The increase in Arg-1 expression was significant with both hydrogel systems. Also consistent with previous observations was an increased Mgl1 expression in co-cultured

WT macrophages. YM1 expression failed to change upon co-culture in both hydrogel systems (Figure 5C).

A significant decrease in TNFα expression for co-cultured macrophage populations was once again observed in collagen systems (Figure 5D). No change in TNFα expression was observed for Matrigel® systems (Figure 5D). Observations of significant increases in IL-10 (Figure 5E) and MCP-1 (Figure 5F) expression upon co-culture were exclusive to Matrigel ® systems. These data suggest that both collagen hydrogel and Matrigel® support a tumor growth environment that promotes an M2-like TAM phenotype. The difference in the expression of selected genes probably reflects the heterogeneity nature of TAMs from different tissue environment.

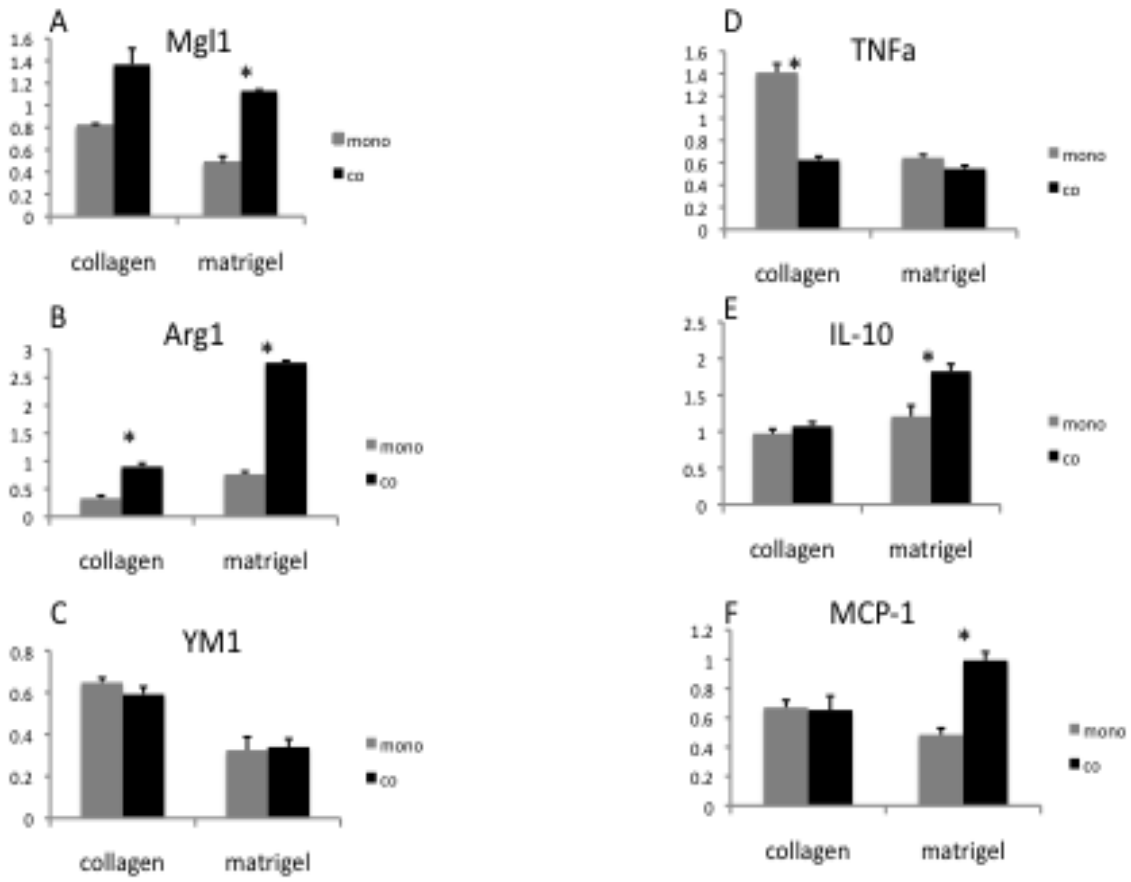

Figure 5. Comparing the effect of culture conditions on gene expression in collagen and Matrigel ® systems. (A) through (F) reflect relative gene expression in WT macrophage populations cultured either alone (gray) or in combination (black) with B16F-10 populations of either hydrogel for a 48 hour period. The "*" symbol reflects a p-value < 0.05.

Chapter IV

Discussion

These findings suggest B16F-10 spheroids are acceptable to serve as a form of tumor in TAMs *in vitro* systems when cultured in a biocompatible 3D hydrogel platform. Gene expression in 2D cultures indicated that B16F-10 exhibit a stronger lipogenic metabolic profile than the B16F-0 line. While 3D culture enhanced this metabolic profile in both melanoma lines, the effect was far more evident in B16F-10 cells. Increased lipogenesis and complex lipid synthesis are established features of cancer metabolism. When paired with the slightly increased proliferative rate observed, increased tumorigenesis in the B16F-10 melanoma line is a logical conclusion. The difference between these two lines is well established. These results are in agreement with previously reported observations.

The co-culture system utilized had a clear and consistent impact on WT macrophage gene expression profiles. Upon review, the majority of melanoma-driven changes in macrophage expression profiles support bias towards an alternatively activated (M2) phenotype. Expression in M2 markers Arg-1 (Figures 3C, 5B) and Mgl1 (Figures 2, 3A, 5A) were shown to be consistently increased in co-cultured populations. Co-culture had the opposite effect on gene expression for M1 marker TNFα (Figures 3D,

5D). MCP-1 expression, like TNFα, is elevated in classically activated (M1) macrophages. We failed to observe any change in MCP-1 expression in response to co-culture (Figure 6F). While consistent, observations reflecting IL-10 and YM1 expression fail to support a tumor driven bias towards either macrophage phenotype. IL-10 and YM1 are both M2 markers. Expression for IL-10 (Figure 5F) and YM1 (Figure 5C) remain unchanged. Induction of Vegfα expression upon co-culture while traditionally the mark of M1 phenotype, is also a widely reported feature of M2-like TAM populations. Angiogenesis is a feature of wound healing and can aid in securing nutrients to support tumor growth. To summarize, M1 markers were either decreased or unaffected while M2 markers were either increased or unaffected. In combination with Vegfα, WT macrophages are not only M2 like, but tumor promoting.

Results reported in Figure 3 reflecting co-culture experiments with STAT6 and PPARδ/γ KO macrophage lines suggest that neither transcriptional regulator is required for the tumor-directed shift in macrophage phenotype. Both KO lines demonstrated the same trends observed in WT gene expression with Mgl1 as well as Arg-1. Additional support is contributed by the observations that both the WT and STAT6 KO macrophages demonstrated significant drops in TNFα expression upon co-culture.

While not required, these transcriptional regulators clearly contribute to the tumorigenic profile in macrophages. While the increased Arg-1 expression in response to co-culture was observed in both KO lines, the effect was slightly stunted. The same can be seen when comparing the decrease in TNFα expression between WT and STAT6KO macrophages. The inability for co-culture of the PPARδ/γKO line to induce a drop in TNFα expression as seen in STAT6KO populations suggests that the manner by which

each transcriptional regulator contributes to the tumor-directed phenotypic shift are not identical.

The preceding conclusions are based on observations from co-culture systems utilizing the customized collagen platform. The results obtained from comparison of this system against Matrigel® 3D culture suggest that while the commercial culture hydrogel may be a better platform for enhancing the tumor-like behavior of 3D melanoma cultures, it's value when incorporated into a co-culture system designed to study TAMs is less evident.

Observations concerning the culture of B16F-10 spheroids clearly demonstrated a capacity to infiltrate Matrigel® hydrogel while little to no infiltration occurred in the mature cultures of collagen coated wells. This is reflected in the images presented in Supplemental Figure 2C versus 2D. This dual form of expansion combining the growth of the principal cellular aggregate with select regions of infiltrative expansion along the periphery better reflect the nature of tumor maturation as expansion and degradation of the ECM surrounding the tumor permit both the continued growth of the tumor as well as space for angiogenesis to feed the growing energetic demands of unabated growth and eventual migration.

Comparisons of 3D culture B16F-10 gene expression further support Matrigel® cultures as a more supportive platform for tumor-like culture growth. Results summarized in Figure 4 suggest a more lipogenic metabolic profile, an established metabolic hallmark of tumor cells, was observed in Matrigel® B16F-10 cultures. Other than Srebp-1c, all lipogenic markers tested increased significantly (FASN) or were found to have a p-value nearly significant (ACC1/ACC2). The combination of Matrigel®

supporting more accurate cancer growth and metabolic activity suggest it more accurately represents melanoma microenvironment then the custom collagen hydrogel.

While the results concerning 3D B16F-10 culture demonstrate Matrigel® may offer an advantage likely the result of a more accurate representation of melanoma microenvironment, findings related how these different forms of culture impacted co-cultured macrophage populations are less clear. Changes in expression profiles upon co-culture were similar between collagen and Matrigel ® systems for Mgl1 (Figure 5A), Arg-1 (Figure 5B) and YM1 (Figure 5C). Increases in gene expression were observed in both systems for Mgl1 and Arg-1, while neither demonstrated a change in YM1 expression. Upon closer examination, the nature of the increased expression for the M2 markers Mgl1 and Arg-1 is greater in Matrigel® systems. These observations, paired with the significant increase in M2 marker IL-10 being exclusive to Matrigel ® systems by themselves would suggest a more polarizing effect is potential with the commercial product than the custom collagen platform.

However, turning our attention to the results concerning macrophage expression of the M1 markers TNFα and MCP-1 reveals that Matrigel® appears to have limitations. Gene expression for the inflammatory signal TNFα decreased upon co-culture with melanoma in collagen systems (Figures 3D, 5D), a result that coincided with our hypothesis of the induction of an M2-like phenotypic profile. The same change was not characteristic in Matrigel® co-culture systems, as Figure 5D demonstrates no change in TNFα expression was observed between mono-cultured and co-cultured WT macrophage populations. MCP-1 is expressed by macrophages as part of the recruitment signaling process of inflammatory response and augments monocyte anti-tumor activity. MCP-1

expression in Matrigel® systems is a concern since significant increase in expression upon co-culture of this M1 marker was exclusive to Matrigel® systems.

These initial findings suggest that Matrigel® 3D culture systems may be better suited for research concerned with the nature of tumor progression, expression profiles, and ECM degradation. While not the primary focus of this experimental design, the limited gene expression profiles and proliferative observations seem to indicate the tumor-like *in vitro* precursor spheroids generated from the B16F-10 cell line may exhibit more tumor-like phenotype in Matrigel® than when paired with the custom collagen platform. In order to verify this, a more comprehensive look at gene expression beyond metabolic profile would need to be investigated. This work also fails to investigate Matrigel's ® potential with any other form of cancer other than melanoma. The relatively basic architecture of ECM in skin offered the best potential for faithful replication in an *in vitro* setting. Our desire for TAMs observations produced in this co-culture platform to translate to in vivo features of cancer maturation meant working with a skin-based system was the best opportunity to limit microenvironmental variance. Based on the limited support behind previously stated conclusion, selection Matrigel ® as the basis for any significant cancer study heavily reliant on in vitro testing would likely not be worth the significant expense it would represent over a in-house produced collagen substitute.

Our experimental design was constructed to compare the two platforms with regards to their ability to serve as the basis for a model for *in vitro* TAMs research. Observations suggest that in cases of initial searches for targets, designs involving a large number of co-culture replicants, or anything where expense is a significant concern when

selecting experimental design that Matrigel® may not offer a clear advantage over a custom collagen platform. Macrophage polarization was biased in the direction of an M2-like phenotype, the characteristic anti-inflammatory features of which are widely accepted as pro-tumorigenic. While the extent of this phenotypic shift may have been greater when the Matrigel® platform was incorporated, the same systems also uniquely demonstrated gene expression characteristics reflecting features that directly contradicted this very potential.

Supplements

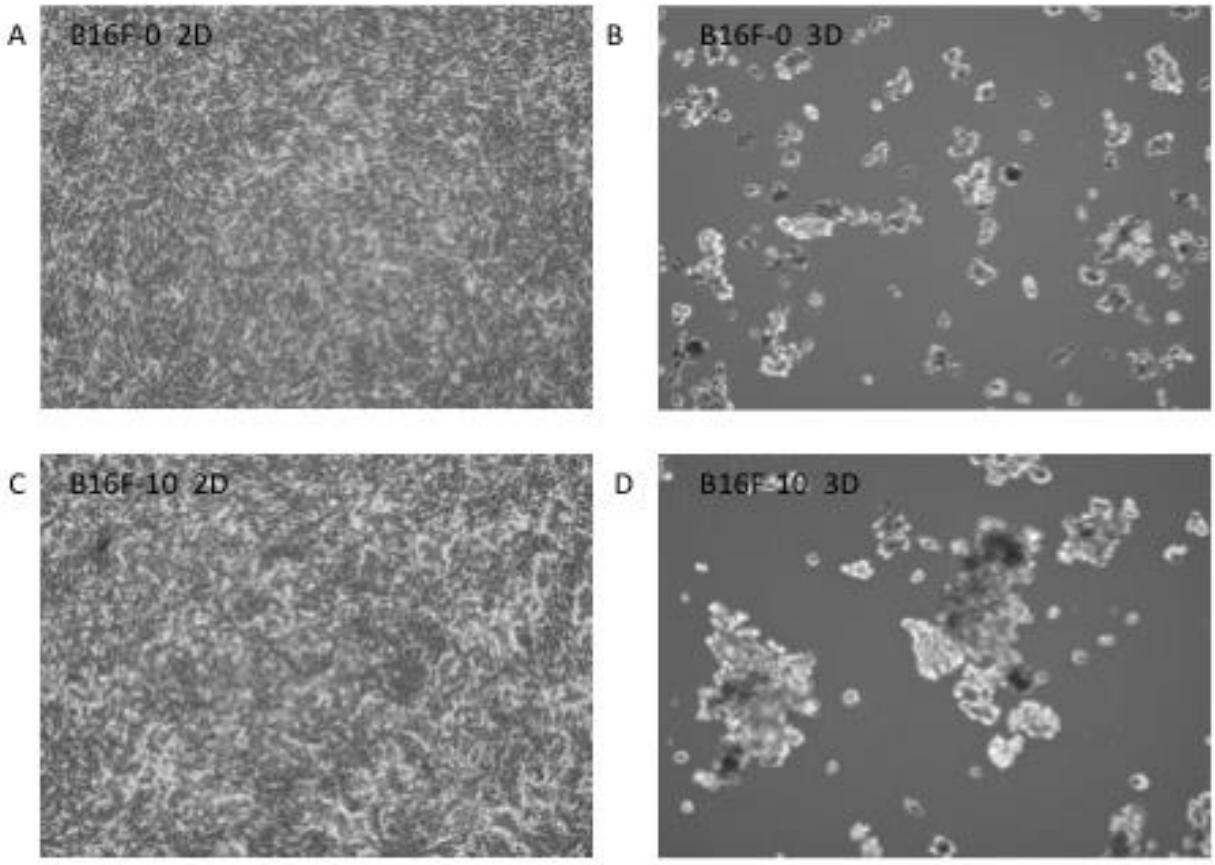

Supplemental Figure 1. Representative images of 2D versus 3D collagen cultures of melanoma lines B16F-0 and B16F-10. Panels (A) and (C) are 2D cell images of F-0 and F-10, respectively, prior to collection. Panels (B) and (D) are 3D collagen culture of F-0 and F-10, respectively, 24 hours post spheroid seeding and prior to start of experimental culture period.

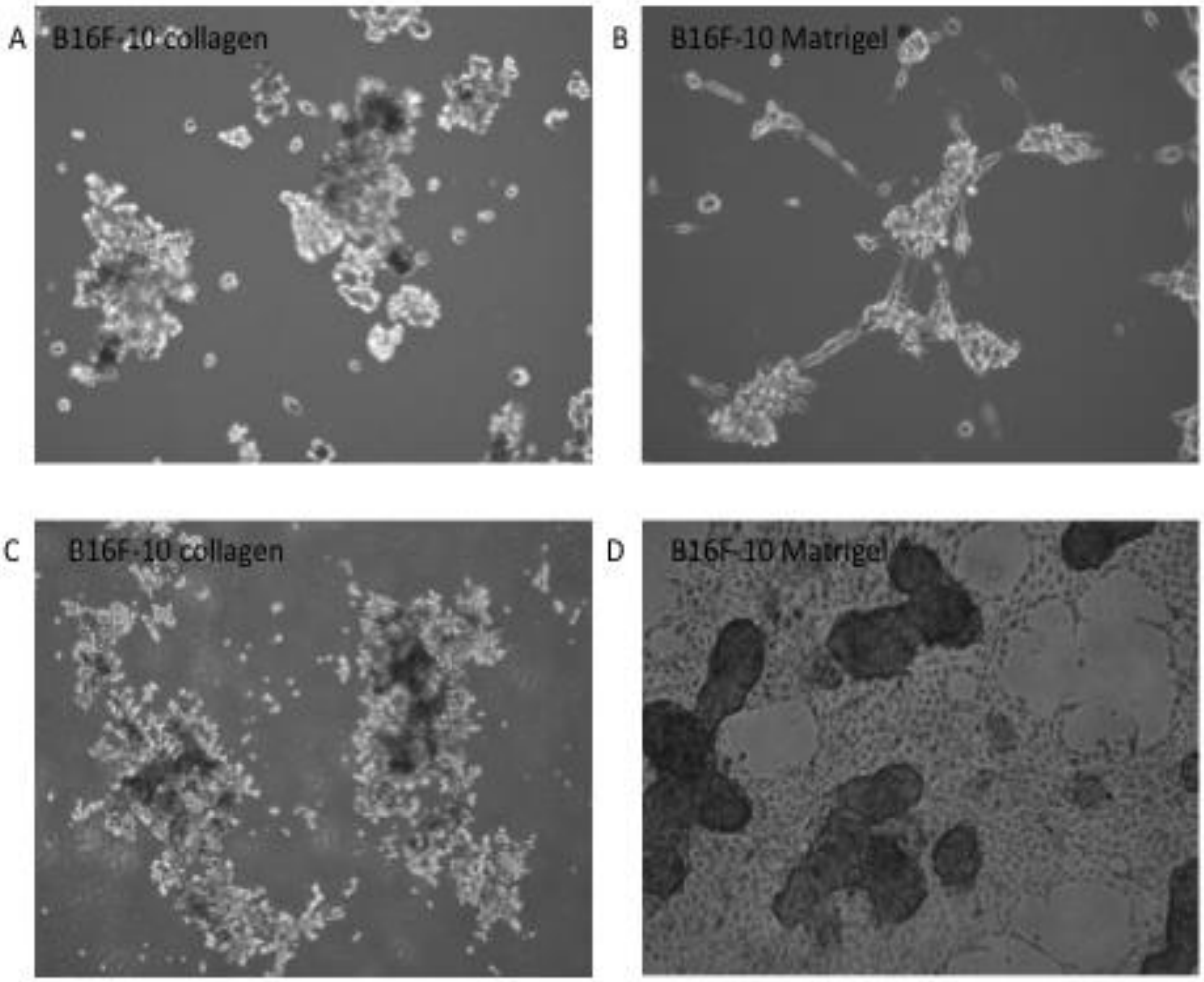

Supplemental Figure 2. Nature of B16F-10 spheroid attachment and maturation in collagen and Matrigel ® cultures. Panels (A) and (B) show melanoma spheroids in collagen and Matrigel ® systems, respectively, after 24 hours of culture. Panels (C) and (D) show the maturation of melanoma populations in collagen and Matrigel ®, respectively, after 36 hours of culture and immediately preceding cell collection.

Gene	F/R	Primer Sequence
36b4	F	AGATGCAGCAGATCCGCAT
36b4	R	GTTCTTGCCCATCAGCACC
ACC1	F	CGCTCGTCAGGTTCTTATTG
ACC1	R	TTTCTGCAGGTTCTCAATGC
ACC2	F	CGCTCACCAACAGTAAGGTGG
ACC2	R	GCTTGGCAGGGAGTTCCTC
Arg-1	F	CTTTGATGTCGATGGGCT
Arg-1	R	CCTGAAAGGAGCCCTGT
FASN	F	AGATGGAAGGCTGGGCTCTA
FASN	R	GGCGTCGAACTTGGAGAGAT
IL-10	F	CTGGACAACATACTGCTAACCG
IL-10	R	GGGCATCACTTCTACCAGGTAA
iNOS	F	GTTCTCAGCCCAACAATACAAGA
iNOS	R	GTGGACGGGTCGATGTCAC
MCP-1	F	CTTCTGGGCCTGCTGTTCA
MCP-1	R	CCAGAATACTCATTGGGATCA
Mgl1	F	GCGAAGCTTACAATGATATACGAAAACCTCC
Mgl1	R	GCGCTCAGACGAGAGCTCCTAGCTCTCC
Srebp-1c	F	GGAGCCATGGATTGCACATT
Srebp-1c	R	GCTTCCAGAGAGGAGGCCAG
STAT6	F	AGCTCAGATATGGGGTATCC
STAT6	R	GCATGGTTATCTGGCTCA
TNFα	F	AAATGGCCTCCCTCTCATCAG
TNFα	R	GTCACTCGAATTTTGAGAAGATGATC
Vegfα	F	TGCAAGGCGAGGCAGCTTGAG
Vegfα	R	TCCCGAAACCCTGAGGGAGGC
YM1	F	AGAAGGGAGTTTCAAACCTGGT
YM1	R	GTCTTGCTCATGTGTGTAAGTGA

Supplemental Table 1. Primer sequences for gene expression. The sequences above were used for primers obtained from IDT and then resuspended for use in RT-PCR. Each sequence is designated as either forward (F) or reverse (R).

References

Baenke, F., Peck, B., Miess, H., & Schulze, A. (2013). Hooked on fat: the role of lipid synthesis in cancer metabolism and tumour development. *Disease Models and Mechanisms, 6*, 1353-1363.

Balkwill, F., Charles, K., & Mantovani, A. (2005). A smoldering and polarized inflammation in the initiation and promotion of malignant disease. *Cancer Cell*, *7*, 211-217.

Bauer, D. E., Hatzivassiliou, G., Zhao, F., Andreadis, C., & Thompson, C. B. (2005). ATP citrate lyase is an important component of cell growth and transformation. *Oncogene, 24*, 6314-6322.

Bauer J., Bahmer, F. A., Wörl, J., Neuhuber, W., Schuler, G., Fartasch, M. (2001). A strikingly constant ratio exists between Langerhans cells and other epidermal cells in human skin: A stereologic study using the optical dissector method and the confocal laser scanning microscope. *The Journal of Investigative Dermatology*, *116*, 313-318.

Bauer, R., Hein, R., & Bosserhoff, A. K. (2005). A secreted form of P-cadherin is expressed in malignant melanoma. *Experimental Cell Research*, *305*, 418-426.

Bingle, L., Brown, N. J. , & Lewis, C. E. (2002). The role of tumor-associated macrophages in tumor progression: implications for new anticancer therapies. *Journal of Pathology*, *196*, 254-265.

Bissell, M. J., & Radisky, D. (2001). Putting tumors in context. *Nature Reviews Cancer*, *1*, 46-54.

Bolós, V., Peinado, H., Pérez-Moreno, M. A., Fraga, M. F., Esteller, M., & Cano, A. (2003). The transcription factor Slug represses E-cadherin expression and induces epithelial to mesenchymal transitions: a comparison with Snail and E47 repressors. *Journal of Cell Science*, *116*, 499-511.

Brown, E. J. (1995). Phagocytosis. *Bioessays*, *17*, 109-117.

Buzzai, M., Bauer, D. E., Jones, R. G., DeBerardinis, R. J., Hatzivassiliou, G., Elstrom, R. L., & Thompson, C. B. (2005). The glucose dependence of Akt-transformed cells can be reversed by pharmacologic activation of fatty acid beta-oxidation. *Oncogene, 24*, 4165-4173.

Cano, A., Pérez-Moreno, M. A., Rodrigo, I., Locascio, A., Blanco, M. J., del Barrio, M. G., Portillo, F.,… Nieto, M. A. (2000). The transcription factor snail controls epithelial-mesenchymal transitions by repression E-cadherin expression. *Nature Cell Biology*, *2*, 76-83.

Cate, D. M., Sip, C. G., & Folch, A. (2010). A microfluidic platform for generation of sharp gradients in open-access culture. *Biomicrofluidics, 4,* 44105.

Charo, I. F. (2007). Macrophage polarization and insulin resistance: PPARgamma in control. *Cell Metabolism*, *6*, 96-98.

Colotta, F., Allavena, P., Sica, A., Garlanda, C., & Mantovani, A. (2009). Cancer-related inflammation, the seventh hallmark of cancer: links to genetic instability. *Carcinogenesis*, *7*, 1073-1081.

Cukierman, E., Pankov, R., & Yamada, K. M. (2002). Cell interactions with three-dimensional matrices. *Current Opinion in Cell Biology*, *14*, 633-639.

Daley, J. M., Brancato, S. K., Thomay, A. A., Reichner, J. S., & Albina, J. E. (2010). The phenotype of murine wound macrophages. *Journal of Leukocyte Biology*, *87*, 59-67.

DeBerardinis, R. J., Lum, J. J., & Thompson, C. B. (2006). Phosphatidylinositol 3-kinase-dependent modulation of carnitine palmitoyltransferase 1A expression regulates lipid metabolism during hematopoietic cell growth. *Journal of Biological Chemistry, 281*, 37372-37380.

Dipietro, L. A., Polverini, P. J., Rahbe, S. M., & Kovacs, E. J. (1995). Modulation of JE/MCP-1 expression in dermal wound repair. *The American Journal of Pathology*, *146*, 868-875.

El Kasmi, K. C., Qualls, J. E., Pesce, J. T., Smith, A. M., Thompson, R. W., Henao-Tamayo, M.,… Murray, P. J. (2008). Toll-like receptor-induced arginase 1 in macrophages thwarts effective immunity against intracellular pathogens. *Nature Immunology*, *9*, 1399-1406.

Eming, S. A., Krieg, T., & Davidson, J. M. (2007). Inflammation in wound repair: molecular and cellular mechanisms. *Journal of Investigative Dermatology*, *127*, 514-525.

Erler, J. T., & Weaver, V. M. (2009). Three-dimensional context regulation of metastasis. *Clinical and Experimental Metastasis*, *26*, 35-49.

Fidler, I. J. (1973). Selection of successive tumour lines for metastasis. *Nature New Biology*, *242*, 148-149.

Fitzpatrick, T. B., & Breathnach, A. S. (1963). Das epidermale Melanin-Einheit system. *Dermatol Wochenschr*, *147*, 481-489.

Fitzpatrick, T. B., & Szabo, G. (1959). The melanocyte; cytology and cytochemistry. *Journal of Investigative Dermatology*, *32*, 197-209.

Gao, S., Mao, F., Zhang, B., Zhang, L., Zhang, X., Wang, M., …Xu, W. (2014). Mouse bone marrow-derived mesenchymal stem cells induce macrophage M2 polarization through the nuclear factor-κB and signal transducer and activator of transcription 3 pathways. *Experimental Biology and Medicine, 239*, 336-375.

Gasic, S., Tian, B., & Green A. (1999). Tumor necrosis factor alpha stimulates lipolysis in adipocytes by decreasing Gi protein concentrations. *Journal of Biological Chemistry*, *274*, 6770-6775.

Geissmann, F., Manz, M. G., Jung, S., Sieweke, M. H., Merad, M., & Ley, K. (2010). Development of monocytes, macrophages, and dendritic cells. *Science*, *327*, 656-661.

Ghajar, C. M., & Bissell, M. J. (2008). Extracellular matrix control of mammary gland morphogenesis and tumorigenesis: insights from imaging. *Histochemistry and Cell Biology, 130*, 1105-1118.

Gil, V., & del Río, J. A. (2012). Analysis of axonal growth and cell migration in 3D hydrogel cultures of embryonic mouse CNS tissue. *Nature Protocols, 7*, 268-280.

Goodhill, G. J., & Baier, H. (1998). Axon guidance: stretching gradients to the limit. *Neural Computation, 10*, 521-527.

Gordon, S., Unkeless, J. C., & Cohn, Z. A. (1974). Induction of macrophage plasminogen activator by endotoxin stimulation and phagocytosis: evidence for a two-stage process. *Journal of Experimental Medicine*, *140*, 995-1010.

Gordon, S. (2007). The macrophage: past, present and future. *European Journal of Immunology*, *37*, Supplemental 9-S17.

Griffith, L. G., & Swartz, M. A. (2006). Capturing complex 3D tissue physiology in vitro. *Nature Reviews Molecular Cell Biology, 7*, 211-224.

Guppy, M., Greiner, E., & Brand, K. (1993). The role of the Crabtree effect and an endogenous fuel in the energy metabolism of resting and proliferating thymocytes. *European Journal of Biochemistry, 212*, 95-99.

Hanahan, D., & Weinberg, R. A. (2011). Hallmarks of cancer: the next generation. *Cell*, *144*, 646-674.

Hatzivassiliou, G., Zhao, F., Bauer, D. E., Andreadis, C., Shaw, A. N., Dhanak, D, …Thompson, C. B. (2005). ATP citrate lyase inhibition can suppress tumor growth. *Cancer Cell, 8*, 311-321.

Hensley, C. T., Wasti, A. T., & DeBerardinis, R. J. (2013). Glutamine and cancer: cell biology, physiology, and clinical opportunities. *Journal of Clinical Investigation, 123*, 3678-3684.

Hirosumi, J., Tuncman, G., Chang, L., Görgün, C. Z., Uysal, K. T., Maeda, K., …Hotamisligil, G. S. (2002). A central role for JNK in obesity and insulin resistance. *Nature*, *420*, 333-336.

Hoath, S. B., & Leahy, D. G. (2003). The Organization of human epidermis: functional epidermal units and Phi proportionality. *The Journal of Investigative Dermatology*. *121*, 1440-1446.

Hosoya, H., Kadowaki, K., Matsusaki, M., Cabral, H., Nishihara, H., Ijichi, H., …Akashi, M. (2012). Engineering fibrotic tissue in pancreatic cancer: A novel three-dimensional model to investigate nanoparticle delivery. *Biochemical and Biophysical Research Communications, 419*, 32-37.

Hübner, G., Brauchle, M., Smola, H., Madlener, M., Fässler, R., & Werner, S. (1996). Differential regulation of pro-inflammatory cytokines during wound healing in normal and glucocorticoid-treated mice. *Cytokine*, *8*, 548-556.

Huang, W. C., Li, X., Liu, J., Lin, J., & Chung, L. W. (2012). Activation of androgen receptor, lipogenesis, and oxidative stress converged by SREBP-1 is responsible for regulating growth and progression of prostate cancer cells. *Molecular Cancer Research, 10*, 133-142.

Huang, S. C., Everts, B., Ivanova, Y., O'Sullivan, D., Nascimento, M., Smith, A. M., …Pearce, E. J. (2014). Cell-intrinsic lysosomal lipolysis is essential for alternative activation of macrophages. *Nature Immunology*, *9*, 846-855.

Ihn, H. (2005). Scleroderma, fibroblasts, signaling, and excessive extracellular matrix. *Current Rheumatology Reports*, *7*, 156-172.

Ishida, Y., Gao, J. L., & Murphy, P. M. (2008). Chemokine receptor CX3CR1 mediates skin wound healing by promoting macrophage and fibroblast accumulation and function. *Journal of Immunology*, *180*, 569-579.

Jones, P. A., & Scott-Burden, T. (1979). Activated macrophages digest the extracellular matrix proteins produced by cultured cells. *Biochemical and Biophysical Research Communications*, *86*, 71-77.

Kalluri, R., & Neilson, E. G. (2003). Epithelial-mesenchymal transition and its implications for fibrosis. *Journal of Clinical Investigation*, *112*, 1776-1784.

Kang, K., Reilly, S. M., Karabacak, V., Gangl, M. R., Fitzgerald, K., Hatano, B., & Lee, C. H. (2008). Adipocyte-derived Th2 cytokines and myeloid PPAR delta regulate macrophage polarization and insulin sensitivity. *Cell Metabolism*, *7*, 485-495.

Keenan, T. M., & Folch, A. (2008). Biomolecular gradients in cell culture systems. *Lab on a Chip, 8*, 34-57.

Kuhajda, F. P., Jenner, K., Wood, F. D., Hennigar, R. A., Jacobs, L. B., Dick, J. D., & Pasternack, G. R. (1994). Fatty acid synthesis: a potential selective target for antineoplastic therapy. *Proceedings of the National Academy of Sciences USA, 91*, 6379-6383.

Laurencikiene, J., van Harmelen, V., Arvidsson Nordström, E., Dicker, A., Blomqvist, L., Näslund, E., …Rydén, M. (2007). NF-kappaB is important for TNF-alpha-induced lipolysis in human adipocytes. *Journal of Lipid Research*, *48*, 1069-1077.

Lazar, M. A., & Birnbaum, M. J. (2012). Physiology. De-meaning of metabolism. *Science, 336*, 1651-1652.

Lee, J. T., & Herlyn, M. (2007). Microenvironmental Influences in Melanoma Progression. *Journal of Cellular Biochemistry*, *101*, 862-872.

Lissbrant, I. F., Stattin, P., Wikstrom, P., Damber, J. E., Egevad, L., & Bergh, A. (2000). Tumor associated macrophages in human prostate cancer: relation to clinicopathological variables and survival. *International Journal of Oncology*, *17*, 445-451.

Lumeng, C. N., Bodzin, J. L., & Saltiel, A. R. (2007). Obesity induces a phenotypic switch in adipose tissue macrophage polarization. *Journal of Clinical Investigation*, *117*, 175-184.

Macdonald, K. P., Palmer, J. S., Cronau, S., Seppanen, E., Olver, S., Raffelt, N. C., …Hume, D. A. (2010). An antibody against the colony-stimulating factor 1 receptor (CSF1R) depletes the resident subset of monocytes and tissue and tumor-associated macrophages but does not inhibit inflammation. *Blood*, *116*, 3955-3963.

Mantovani, A., & Sica, A. (2010). Macrophages, innate immunity and cancer: balance, tolerance, and diversity. *Current Opinions in Immunology*, *22*, 231-237.

Melnikova, V. O., Bolshakov, S. V., Walker, C., & Ananthaswamy, H. N. (2004). Genomic alterations in spontaneous and carcinogen-induced murine melanoma cell lines. *Oncogene*, *23*, 2347-2356.

Mirza, R., Dipietro, L. A., & Koh, T. J. (2009). Selective and specific macrophage ablation is detrimental to wound healing in mice. *The American Journal of Pathology*, *175*, 2454-2462.

Mosser, D. M., & Edwards, J. P. (2008). Exploring the full spectrum of macrophage activation. *Nature Reviews Immunology*, *8*, 958-969.

Nakamura, K., Yoshikawa, N., Yamaguchi, Y., Kagota, S., Shinozuka, K., & Kunitomo, M. (2002). Characterization of mouse melanoma cell lines by their mortal malignancy using an experimental metastatic model. *Life Sciences*, *70*, 791-798.

Nelson, C. M., Vanduijn, M. M., Inman, J. L., Fletcher, D. A., & Bissell, M. J. (2006). Tissue geometry determines sites of mammary branching morphogenesis in organotypic cultures. *Science, 314*, 298-300.

Oh, J., Riek, A. E., Weng, S., Petty, M., Kim, D., Colonna, M., …Bernal-Mizrachi, C. (2012). Endoplasmic reticulum stress controls M2 macrophage differentiation and foam cell formation. *Journal of Biological Chemistery*, *287*, 11629-11641.

Park, S. J., Kim, Y. T., & Jeon, Y. J. (2012). Antioxidant dieckol downregulates the Rac1/ROS signaling pathway and inhibits Wiskott-Aldrich syndrome protein (WASP)-family verprolin-homologous protein 2 (WAVE2)-mediated invasive migration of B16 mouse melanoma cells. *Molecules and Cells*, *33*, 363-369.

Pena, O. M., Pistolic, J., Raj, D., Fjell, C. D., & Hancock, R. E. (2011). Endotoxin tolerance represents a distinctive state of alternative polarization (M2) in human mononuclear cells. *Journal of Immunology, 186*, 7243-7254.

Pesce, J. T., Ramalingam, T. R., Mentink-Kane, M. M., Wilson, M. S., El Kasmi, K. C., Smith, A. M., …Wynn, T. A. (2009). Arginase-1-expressing macrophages suppress Th2 cytokine-driven inflammation and fibrosis. *PLoS* Pathog 5(4): e1000371. doi:10.1371/journal.ppat.1000371.

Pizer, E. S., Wood, F. D., Heine, H. S., Romantsev, F. E., Pasternack, G. R., & Kuhajda, F. P. (1996). Inhibition of fatty acid synthesis delays disease progression in a xenograft model of ovarian cancer. *Cancer Research, 56*, 1189-1193.

Pollard, J. W. (2004). Tumor-educated macrophages promote tumor progression and metastasis. *Nature Reviews Cancer*, *4*, 71-78.

Rodriguez, P. C., Quiceno, D.G., Zabaleta, J., Ortiz, B., Zea, A. H., Piazuelo, M. B., …Ochoa, A.C. (2004). Arginase I production in the tumor microenvironment by mature myeloid cells inhibits T-cell receptor expression and antigen-specific T-cell responses. *Cancer Research*, *64*, 5839-5849.

Rommerswinkel, N., Niggemann, B., Keil, S., Zänker, K. S., & Dittmar, T. (2014). Analysis of cell migration within a three-dimensional collagen matrix. *Journal of Visualized Experiments, 92*, e51963, doi:10.3791/51963.

Rosoff, W. J., McAllister, R., Esrick, M. A., Goodhill, G. J., & Urbach, J. S. (2005). Generating controlled molecular gradients in 3D gels. *Biotechnology and Bioengineering, 91*, 754-759.

Ross, R., Everett, N. B., & Tyler, R. (1970). Wound healing and collagen formation. VI. The origin of the wound fibroblast studied in parabiosis. *Journal of Cell Biology*, *44*, 645-654.

Sabuncu, A. C., Liu, J. A., Beebe, S. J., & Beskok, A. (2010). Dielectrophoretic separation of mouse melanoma clones. *Biomicrofluidics*, 4, doi:10.1063/1.3447702.

Sarraf, P., Mueller, E., Jones, D., King, F. J., DeAngelo, D. J., Partridge, J. B., …Spiegelman, B. M. (1998). Differentiation and reversal of malignant changes in colon cancer through PPARgamma. *Nature Medicine, 4*, 1046-1052.

Sato, H., Ishihara, S., Kawashima, K., Moriyama, N., Suetsugu, H., Kazumori, H., …Kinoshita, Y. (2000). Expression of peroxisome proliferator-activated receptor (PPAR)gamma in gastric cancer and inhibitory effects of PPARgamma agonists. *British Journal of Cancer, 83*, 1394-1400.

Schäfer, M., & Werner, S. (2008). Cancer as an overhealing wound: an old hypothesis revisited. *Nature Reviews*. *Molecular Cell Biology*, *9*, 628-638.

Shulz, C., Gomez-Perdiguero E., Chorro, L., Szabo-Rogers, H., Cagnard, N., Kierdorf, K., …Geissmann, F. (2012). A lineage of myeloid cells independent of Myb and hematopoietic stem cells. *Science*, *336*, 86-90.

Shapiro, S. D., Kobayashi, D. K., & Ley, T. J. (1993). Cloning and characterization of a unique elastolytic metalloproteinase produced by human alveolar macrophages. *Journal of Biological Chemistery*, *268*, 23824-23829.

Solinas, G., Germano, G., Mantovani, A., & Allavena, P. (2009). Tumor-associated macrophages (TAM) as major players of the cancer-related inflammation. *Journal of Leukocyte Biology*, *86*, 1065-1073.

Teupser, D., Burkhardt, R., Wilfert, W., Haffner, I., Nebendahl, K., & Thiery, J. (2006). Identification of macrophage arginase I as a new candidate gene of atherosclerosis resistance. *Arteriosclerosis, Thrombosis, and Vascular Biology*, *26*, 365-371.

Thomas, A. C., Sala-Newby, G. B., Ismail, Y., Johnson, J. L., Pasterkamp, G., & Newby, A. C. (2007). Genomics of foam cells and nonfoamy macrophages from rabbits identifies arginase-I as a differential regulator of nitric oxide production. *Arteriosclerosis, Thrombosis, and Vascular Biology*, *27*, 571-577.

Timpl, R., & Brown, J. C. (1996). Supramolecular assembly of basement membranes. *Bioessays*, *18*, 123-132.

Vats, D., Mukundan, L., Odegaard, J. I., Zhang, L., Smith, K. L., Morel, C. R., …Chawla, A. (2006). Oxidative metabolism and PGC-1beta attenuate macrophage-mediated inflammation. *Cell Metabolism*, *4*, 13-24.

Vogler, R., Sauer, B., Kim, D. S., Schäfer-Korting, M., & Kleuser, B. (2003). Sphingosine-1-phosphate and its potentially paradoxical effects on critical parameters of cutaneous wound healing. *Journal of Investigative Dermatology*, *120*, 693-700.

Warburg, O. (1925). Uber den Stoffwechsel der Carcinomzelle. *Klinische Wochenschrift, 4*, 534-536.

Warburg, O. (1956a). On respiratory impairment in cancer cells. *Science, 124*, 269-270.

Warburg, O. (1956b). On the origin of cancer cells. *Science, 123*, 309-314.

Watt, F. M., & Fujiwara, H. (2011). Cell-extracellular matrix interactions in normal and diseased skin. *Cold Spring Harbor Perspectives in Biology*, 3:a005124.

Weisberg, S. P., McCann, D., Desai, M., Rosenbaum, M., Leibel, R. L., & Ferrante Jr., A.W. (2003). Obesity is associated with macrophage accumulation in adipose tissue. *Journal of Clinical Investigation*, *112*, 1796-1808.

Weitkamp, B., Cullen, P., Plenz, G., Robenek, H., & Rauterberg, J. (1999). Human macrophages synthesize type VIII collagen *in vitro* and in the atherosclerotic plaque. *Federation of American Societies for Experimental Biology Journal*, *13*, 1445-1457.

Werner, S., & Grose, R. (2003). Regulation of wound healing by growth factors and cytokines. *Physiological Reviews*, *83*, 835-870.

Xu, H., Barnes, G. T., Yang, Q., Tan, G., Yang, D., Chou, C. J., …Chen, H. (2003). Chronic inflammation in fat plays a crucial role in the development of obesity-related insulin resistance. *Journal of Clinical Investigation*, *112*, 1821-1830.

Yoon, S., Lee, M. Y., Park, S. W., Moon, J. S., Koh, Y. K., Ahn, Y. H., …Kim, K. S. (2007). Up-regulation of acetyl-CoA carboxylase alpha and fatty acid synthase by human epidermal growth factor receptor 2 at the translational level in breast cancer cells. *Journal of Biological Chemistry, 282*, 26122-26131.

Zea, A. H., Rodriquez, P. C., Atkins, M .B., Hernandez, C., Signoretti, S., Zabaleta, J., …Ochoa, A.C. (2005). Arginase-producing myeloid suppressor cells in renal cell carcinoma patients: a mechanism of tumor evasion. *Cancer Research*, *65*, 3044-3048.